5-5-2020

Investigation of Rapid Diagnostic Tests for Characterization of Mycobacterium Avium Complex (MAC) from various isolates and Identification of Virulence Factors of Porcine Reproductive and Respiratory Syndrome Virus (PRRSV) in Vitro

Claudia Antonika
University of Nebraska - Lincoln, claudia.antonika@gmail.com

Investigation of Rapid Diagnostic Tests for Characterization of Mycobacterium Avium Complex (MAC) from various isolates and Identification of Virulence Factors of Porcine Reproductive and Respiratory Syndrome Virus (PRRSV) *in Vitro*

An Undergraduate Honor Thesis presented in Partial Fulfillment of Degree of Distinction Requirement in the College of Agricultural and Natural Sources (CASNR)

By

Claudia Natasha Antonika, BS

Microbiology

Department of Plant Pathology

Faculty Advisors:

Dr. Hiep Vu, DVM, PhD, Department of Animal Science
Dr. John Dustin Loy, DVM, PhD, School of Veterinary Medicine and Biomedical Sciences
Dr. Sarah Sillman, DVM, PhD, School of Veterinary Medicine and Biomedical Sciences

Acknowledgement

First and foremost, I would like to express my gratitude towards my primary advisors: Dr. John Dustin Loy and Dr. Hiep Lai Xuan Vu for mentoring me throughout this research process and supporting me to become a better researcher. I also appreciate the extensive guidance from my co-advisors: Dr. Raul Barletta for examining my research and Dr. Sarah Sillman for overseeing this thesis. Furthermore, I want to extend my thanks towards other staff and student assistants who have helped me in these past two years of mycobacteria research at the UNL Veterinary Diagnostic Center: Caitlyn Deal, Shalyn Miller, Aaron Knapp, Erin Weaver, Jamie Bauman, Austin Pierce, and Kara Robbins. An additional thank you for Dr. Matthew Hille, who assisted me in developing a novel FT-IR sample preparation, and Denise Zinniel from Barletta's lab, who guided me in the media preparation. For the virology project in Dr.Vu's lab, I would like to thank Jayesh Chaudhari, a PhD student, for his patience while teaching me complex virology research techniques, and Dr. Fernando Osorio for providing feedback for my thesis development. The funding for mycobacteria research was partially supported by the Nebraska Agricultural Experiment Station with funding from the Animal Health and Disease Research (Section 1433) capacity funding program (Accession Number 1017646) from the USDA National Institute of Food and Agriculture. Extra funding was given through UCARE (Undergraduate Creative and Research Experiences Program) and an IANR (Institute of Agricultural and Natural Sources) Undergraduate Research Grant. In addition, the strains of Mycobacteria were gifted from Dr. Michael Collins from the University of Wisconsin-Madison.

Table of Contents

General Abstracts

Chapter 1

Mycobacterium avium complex (MAC) has become one of the major problems in public health and livestock. Members of MAC, such as *M. avium* subsp *paratuberculosis* (MAP) and *M. avium* subsp *hominissuis* (MAH), are responsible for many opportunistic infections and the loss of livestock. MAP is economically significant to the beef and dairy industries because it is the etiologic agent of Johnes's disease, a chronic and fatal enteritis in ruminants. Tracing the infection sources of MAC could be difficult since it infects many types of hosts in the natural environment. Furthermore, there is less information known about MAP pathogenicity in specific hosts, but some strains often predominate in certain hosts. Being able to differentiate subspecies of MAC, as well as to trace MAP host species of origin, would be important tools for researchers to assess the potential pathogenicity, transmissibility, and environmental persistence of the strains to limit outbreaks. Thus, this study aimed to characterize *M. avium* subspecies and to identify MAP host species of origin using MALDI TOF MS (Matrix Assisted Laser Desorption/Ionization- Time of Flight Mass Spectrometry) library and FT-IR (Fourier Transform-Infrared Spectroscopy) biomarker based proteomic approaches. MALDI-TOF MS provided more sensitive characterization of MAC subspecies through matching mass fingerprint of isolates with a custom main consensus library (MSP). The manufacturer's database (BDAL) discriminated 14 out of 47 MAC isolates (29 %). Our new data database (MSP) could identify 80% of the total isolates (40/47). Our Kappa Analysis was 0.73, signifying good agreement between the PCR and MALDI-TOF results. The FT-IR offered visualization of unique IR spectra that could be analyzed based on the cell wall components present in the cell, such as mycolic acid and peptidoglycan. Both instruments could successfully classify each subspecies of MAC, but it failed to track the host origin of species of MAC.

Chapter 2

Porcine reproductive and respiratory syndrome (PRRS) is a major viral disease responsible for huge economic losses and morbidity in the swine industry. Clinical signs of PRRS include chronic respiratory disease among young pigs and reproductive failure of pregnant sows. The etiologic agent of PRRS is a member of *Arterivirus*, and known as PRRS virus (PRRSV). There are two types of PRRSV circulating worldwide, classified as PRRSV-1 (European) and PRRSV-2 (North American). Genetic variations among PRRSVs are common as their RNA genome is prone to mutation. Multiple types of vaccines have been created, including a synthetic vaccine candidate (PRRSV-CON) which can provide broader protection against the two types of PRRSV (Vu et al., 2015). Nevertheless, the mechanism of how PRRSV provides immune protection remains unclear regarding which viral proteins trigger optimum immune responses. Hence, in this project, our goal was to determine the relative contribution of PRRSV-2 structural proteins located in Open Reading Frames (ORFs) 2-7 to immune responses. We used PRRSV-1 as a backbone for our construct and inserted PRRSV-2 structural proteins. Our construct was not successfully recovered in the cell culture, possibly because the replacement of ORF2-7 from a divergent genotype may interfere with viral replication.

A. Chapter 1

1. Background and Literature Review

1.1 Characteristics of *Mycobacterium avium* complex (MAC)

1.1.1 Taxonomy and Phylogenetics

Mycobacterium avium complex (MAC) is a part of genus *Mycobacterium* in the family of *Mycobacteriaceae*. MAC is a group of organisms consisting of two major species: *Mycobacterium avium* and *Mycobacterium intracellulare*. *M. avium* is further categorized into four subspecies: *M. avium* subsp. *paratuberculosis* (MAP), *M. avium* subsp. *hominissuis* (MAH), *M. avium* subsp. *silvaticum* (MAS), *M. avium* subsp. *avium* (MAA), as is shown in *Figure 1* (Biet et al., 2005). The classification of these subspecies is based on whole genome sequence analysis of 16s and 23s ribosomal RNA internal transcribed spacer (ITS) (Mijs et al., 2002). Furthermore, the subspecies classification is also dependent on the host range. Each of the *M. avium* subspecies often predominates certain hosts; for instance, MAP and MAH are often isolated in swine and humans, while the other two subspecies are commonly found in birds (Rathnaiah et al., 2017). The genetic diversity of MAC is high, which was confirmed in a study from Arbeit *et al* finding that there were 10 different serovars of MAC found in samples from AIDS patients. Likewise, analysis of restriction fragment length polymorphisms (RFLP) provided different genetics sequence patterns between MAC strains in AIDS and non-AIDS patients (Arbeit et al., 1993). Internal multidrug resistance genes for MAC are known to be pks 12 and maa 2520. Pks 12 is a gene related to cell permeability and maa 2520 is associated with cell surface proteins. The presence of these two genes in MAC will increase resistance toward drugs such as ciprofloxacin, clarithromycin, and penicillin by inhibiting drug penetration into the cells (Philalay et al., 2004).

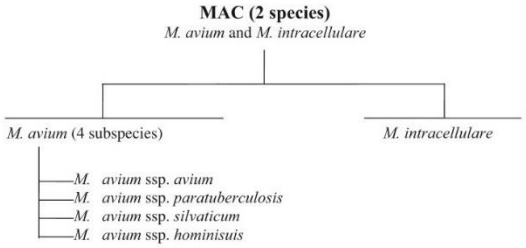

Phylogenetics of MAC (Biet et al., 2005)

1.1.2 Physical Characteristics

MAC members are gram positive, acid-fast, and facultative intracellular aerobes. These bacteria are small, non-motile rod shapes, and non-spore forming, with a size of (0.5 × 1.5 μm). MAC is also characterized by slow-growing bacteria with a generation time of 20 hours The cell walls of MAC have a lipid content of 60%, creating a highly hydrophobic environment with low permeability. Most of the lipid makes up the mycolate portions. The peptidoglycan portions are bounded by arabinogalactan, which is the integral part of cell wall formation. The synthesis of MAC cell walls, particularly MAP, is complex and dependent on the essential growth factors. Initial attempts to grow MAP *in vitro* initially failed because growth requires mycobactin J, an iron-binding siderophore. This occurred because MAP has lost its *mbtA* gene in the mycobactin synthesis operon(Biet et al., 2005).

1.1.3 Virulence Factors

Most members of MAC are opportunistic pathogens with several virulence factors. One key virulence factor of MAC is lipoarabinomannan (LAM) located in the outer surface of the cells. LAM suppresses immune responses by inhibiting IFN-γ induction and cytokines of macrophages. The mycolic acid of MAC is immunogenic and toxic in mammalian cells. These characteristic features facilitate MAC survival in unfavorable conditions and the presence of antibiotics(Philalay et al., 2004). In general, the virulence factors of MAC are due to the

organisms' ability to survive inside macrophages. MAC resists the acidification of macrophages and inhibits Rab7 protein, which is important for fusion of phagosome and lysosome. Furthermore, a study from Li *et al*, suggests that PPE and PE gene families, encoding for numerous unknown proteins, contribute to the virulence of MAC, as mutants of these genes can't prevent the fusion of lysosomes and phagosomes in macrophages (Li et al., 2010).

1.1.4 Pathogenesis of MAC

The survival strategy of MAC is based on their ability to escape from the host defense. MAC activates mitogen-activated protein kinase (MAPK) pathway to upregulate interleukin 10 (IL-10). As a result, increased IL-10 blocks phagosome maturation. Thus, MAC can maintain survive inside the host cells (Hussain et al., 2016). High concentration of IFN-γ and granulocyte macrophage-colony stimulating factor can also inhibit intracellular growth of MAC in the bovine monocytes (Rathnaiah et al., 2017). In addition, in a complimentary experiment by Rathnaiah *et al*, murine macrophage cell lines treated with high level of TNF-α produced lower recovery of viable MAC.

The pathogenesis of MAC is likely influenced by nutritional status in animals. An experiment with mice showed a reduced amount of dietary calcium could suppress MAC infection (Rathnaiah et al., 2017). Iron availability is also a significant factor since it is required for the cytochromes to transport electrons, and it is involved in oxygen metabolism of other hemoproteins, such as catalase-peroxidase KatG (de Voss et al., 1999). The majority of MAC hosts restrict the ability of MAC to harvest iron. In an activated macrophage, transferrin receptors are downregulated to limit the concentration of free iron (Wang et al., 2015). To overcome this, most of the mycobacterial species produce lipid-soluble mycobactin and water soluble siderophore exochelin (Rathnaiah et al., 2017). These features are significant in the

virulence factors of MAC to enable iron acquisition. Interestingly, MAP only produces exochelin, and little is known about how it survives without mycobactin.

1.2 Epidemiology

1.2.1 Transmission of MAC

The exposure of MAC to humans can come from various routes. This includes natural biotopes like insects and protozoa or contaminated food and shedding. Birds are the major agent of transmission as they can transmit MAC through feces for broader distances (Rathnaiah et al., 2017). Once MAC contaminates soil and environment, it is difficult to eliminate as it can persist for long periods of time. Thus, most of the transmission in ruminants and livestock is due to fecal contamination of MAP from wildlife and environment (Biet et al., 2005).

1.2.2 Variable Genetic Elements

MAC members are diverse and are difficult to differentiate. However, molecular epidemiology with RFLP is able to differentiate members of MAC from different hosts (Rebuffo-Scheer et al., 2007). It is suspected that the strains may undergo adaptation. A study using RFLP analysis found MAP in sheep and MAP in cattle are distinct(Roiz et al., 1995). Moreover, insertion sequences that are specific to MAC are often used for epidemiological analysis. Insertion sequences are a mobile genetic element, having transposition function. The family of MAC insertion sequences have a specific feature of lacking both terminal inverted repeats in their insertion sequences (IS). There are four IS found belonging to MAC: IS 900 for MAP, IS 901 MAA, IS 902, MAS, IS 1110 for MAA and MAI (Kunze et al., 1992).

1.2.3 Host Ranges

The host ranges of MAC are diverse in the environment and wildlife due to their flexibility to adapt in various conditions. Birds and ruminants are the most common reservoirs

harboring MAC. Interestingly, MAC also infects insect and protozoa (Biet et al., 2005). Little is known about how MAC dominates in a certain host. Nevertheless, host adaptation can change the microbial morphology. The fatty acid (FA) profiles between MAP infecting sheep are different from MAP infecting cattle. This implies that FA composition may affect the survival of MAP in different host macrophages (Alonso-Hearn et al., 2017).

1.3 Clinical Diseases, Treatments, Impacts

1.3.1 Clinical Diseases

Johne's disease causes a severe chronic enteritis, primarily caused by MAP, a member of MAC. It is highly contagious among ruminants, and the transmission of the pathogen often goes unnoticed until the clinical signs develop well after exposure and initial infection. In the US, dairy herds have been reported to have very high prevalence of Johne's disease. It could approach to 100 % herd level prevalence among large herds (McNees et al., 2015). The clinical signs of Johne's disease in cattle include diarrhea and weight loss with normal appetite. After the establishment of diarrhea, the cattle will develop "bottle jaw." This occurs because proteins are lost from bloodstream to the digestive tract (protein losing enteropathy). As a result, it will cause edema in its jaw due lowered oncotic pressure within blood plasma. At this stage, the survival rate is very low, and the infection may have spread widely in the herd. For sheep and goats, the clinical signs are even harder to notice. Usually, the infected sheep will have normal appetite, but it loses a lot of weight because the intestine fails to absorb nutrients. However, diarrhea is rarely observed in sheep in contrast to cattle. As the clinical diseases progress, the shedding increases. Thus, it enhances the risk of transmission.

MAP is also suspected to have association with an inflammatory bowel disease, commonly called Crohn's disease (CD) in humans (McNees et al., 2015). Crohn's disease is

parallel to Johne's disease as it affects digestive system. The signs and symptoms of Crohn's disease in humans are abdominal pain, diarrhea, and blood in the stool It was thought that Crohn's disease was an autoimmune disease. Several attempts to culture MAP was unsuccessful until Naser *et al* did culture MAP. His study suggests that MAP contributes to Crohn's disease. Furthermore, PCR tests of Crohn's disease patients show positive results of MAP DNA. This result together with Meta-analysis data confirmed the present of MAP DNA in Crohn's disease patients. Hence, there is a strong linkage between MAP and Crohn Disease (Naser et al., 2014).

1.3.2 Economic Impacts

In the United States, the economic impacts of Johne's disease are significant to the dairy and beef industries. The losses are mostly attributed due to reduced milk production, premature culling, and weight loss at slaughter. For Johne's-positive herds, the industry could lose approximately $100 per head (Ott et al., 1999). The production of milk can be reduced up to 700 kg/head for high-prevalence herds. Several reports have estimated the annual loss due to Johne's disease in regions, such as in New England at $15.4 million, $54 million in Wisconsin, $5.4 million in Pennsylvania, and $200 million to up to $250 million loss annually throughout the US. In comparison, in Australia, the loss is estimated to be $2.1 million (Garcia & Shalloo, 2015).

1.3.3 Treatments

Since there are no clinical signs observed in the initial infection of MAP, it is very hard to control MAP transmission. Hence, early detection of MAP is the best practice to prevent Johne's disease (JD). Treatments for JD are mostly ineffective as the majority of MAP are resistant to therapy (Philalay et al., 2004). Vaccines are currently available, but they are limited and do not give long term protection against JD. For instance, a licensed vaccine, Mycopar, is produced from protein derived MAA strains. Thus, it does not give optimum responses against MAP or

other MAC variants (Bastida & Juste, 2011). Moreover, In Australia, heat-killed vaccine made from MAP 316F strains could provide better immunity, but the vaccine compromises JD diagnosis tests, make it difficult to detect between vaccinated and unvaccinated animals (Mancini et al., 2013).

JD treatments with antibiotics could be effective, but it is never encouraged for economic reasons because it is highly unlikely the animals can be cured, and the cost of the antibiotic is expensive. In addition, the consequences of long-term antibiotic treatment may affect the production of milk and meat, and it may not pass the USDA regulations as the drug may not be proper for human consumption (Philalay et al., 2004). It has been demonstrated that macrolide drugs, such as clarithromycin and azithromycin, have potent efficacy *in vitro*, while anti-tuberculosis and anti-leprosy drugs are not effective against MAP with exception of rifampicin family (Krishnan et al., 2009). These results do not correspond to the *in vivo* results. When the drugs were tested in cattle infected with MAP. There was only 50% of success rate with antibiotic treatments. Hence, antibiotic therapy is not the best way to treat JD (Krishnan et al., 2009).

1.4 Diagnostic Tests

Various diagnostic tests have been developed for early detection of MAP. The most common diagnostic tests include Polymerase Chain Reaction (PCR), isolation of MAP by culture, and direct acid-fast staining of clinical samples. Usually the initial screening of MAP is done with acid-fast staining because it is fast, simple, and cheap. However, due to lack of specificity, further screening by PCR or immunoassay is needed to confirm the specificity of MAP. The "gold standard" for JD diagnosis is isolation of MAP culture in lab. Since it is known that MAP is dependent on the presence of mycobactin, it is very easy to distinguish between those MAP

and non-MAP in the media lacking mycobactin. However, this method is not practical in terms of the lengthy process to grow the culture for 6-8 weeks (Krishnan et al., 2009). PCR assay provides more a rapid and sensitive diagnosis. The assay uses primer IS900, an insertion element that is specific to MAP, but a study suggests that it may give false positive results as the insertion element is also present in other species of mycobacteria(Erume et al., 2001).

1.4.1 Matrix Assisted Laser Desorption ionization-time of flight mass spectrometry (MALDI-TOF MS)

Current emerging technologies have been able to differentiate MAC and detect MAP in rapid and cost-efficient ways (Singhal et al., 2015). MALDI-TOF Biotyper is one example of a technology platform developed in Germany by Bruker Daltonik to characterize and compare mass fingerprints from microbiological samples. This instrument uses an analytical method of mass spectrometry where the samples are crystallized and ionized into charged ions, and their mass to charge ratios are measured. Unlike the regular mass spectrometry in the chemical sciences, MALDI-TOF Biotyper utilizes matrix assisted laser desorption ionization (MALDI) to detect larger molecules like proteins. Peptides are ionized by the addition or loss of one or more protons. Thus, this soft ionization will not cause huge loss in the sample integrity. One major advantage of MALDI-TOF MS is that it does not require sample separation by chromatography, and the samples can be applied directly for MALDI-TOF analysis. In addition, it also produces single charged ions, providing easier interpretation for the samples results.

The principle of MALDI-TOF MS is similar to regular mass spectrometry with an exception to the preparation methods. The samples for MALDI-TOF MS require an energy absorbent reagent from organic compound called matrix to coat the samples. This matrix will crystallize the sample after drying, and it will trap the analyte inside the crystal (Singhal et al.,

2015). The crystallized matrix will be ionized by a laser beam. A single ion from analytes of the samples will be generated. Then, the protonated ions will move at fixed potential, where they separate based on their mass to charge ratio (m/z). The mass analyzer and TOF (time of flight) analyzer will detect the movement of protonated ions. The m/z ratio will be measured based on the time required for the protonated ions to move to the length of the flight tubes. Some TOF analyzers have an ion mirror at the rear end of the flight tubes. The function of this feature is to correct small differences in energy among ions by reflecting the ions from the flight tubes to the detector. The MALDI-TOF device work in tandem with computer software to do analysis that will display characterized spectra called peptide mass fingerprint (PMF) from analytes of the samples (Croxatto et al., 2012a).

To identify microbes, the PMF of the unknown microbes will be matched with the PMFs of microbes stored in databases, or another option is to match the PMF of unknown microbes with a proteomic database (Murray, 2012). Identification of microbes at the species level is driven mainly by the detection of highly abundant ribosomal proteins and some housekeeping proteins with typical mass range of 2-20 kDa.

There are several sample preparation methods that have been developed for MALDI-TOF Biotyper analysis, and these may depend on the nature of the microbes. Some microbes may require more complicated sample preparations to ensure adequate peptide liberalization and ionization. The easiest and fastest method is the direct smear method, in which a colony of bacteria is collected and spotted onto MALDI target plate with a sterilized toothpick and left to dry for few minutes before coating it with the matrix. HCCA (α-cyano-4-hydroxycinnamic acid), 2,5-dihydroxy benzoic acid (DHB), and 3,5-dimethoxy-4-hydroxycinnamic acid (sinapinic acid) are matrices commonly used for microbiological samples as they have been proven to be the

most efficient (de Alegría Puig et al., 2017). These matrices contain water and organic solvents, such as ethanol, acetonitrile, or trifluoro acetic acid (TFA), which help to dissolve the cell wall of microbes and extract the intracellular components. As the solvent dries, the matrices will co-crystallize with the intracellular components. For complex microorganisms, an extra preparatory extraction is required to maximize the PMF generation. Addition of formic acid could increase the PMF quality of Gram-positive bacteria, but not in Gram-negative bacteria (Alatoom et al., 2011). For mycobacteria, heat killing in 95° Celsius heat bath and longer vortexing with zirconia silica bead are necessary to lyse and extract the intracellular protein as these bacteria have waxy layers (Saleeb et al., 2011).

It has been reported that the culture conditions do not affect microbial identification by MALDI-TOF MS although it changes microbial physiology and the protein expression. Carbonelle *et al* cultured distinct condition with distinct culture time, and it did not influence the result of MALDI-TOF identification (Carbonnelle et al., 2007).

Application of MALDI-TOF is not limited to detection of bacteria. It can identify a broad range of microorganisms such as viruses and fungi, and it can also detect antimicrobial resistance phenotypes. Croxatto *et al*. reported that MALDI-TOF MS could discriminate *S. aureus* with methicillin resistance (Croxatto et al., 2012a). There is a shift in the PMF for resistant microbes. For instance, in β-lactam resistant bacteria, the bacteria produce the enzyme β-lactamase to hydrolyze β-lactams. This can be detected by MALDI-TOF MS with a specific assay called "mass spectrometric β-lactamase (MSBL) assay." To prepare this assay, both antibiotic and the bacteria are mixed in the culture and incubated. Afterwards, the mixture is centrifuged, and the supernatant is taken for MALDI-TOF MS analysis. The PMF generated will shift from non-hydrolyzed to hydrolyzed form of β-lactam. Hence, it can identify the presence or absence of β-

lactam resistant bacteria (Hooff et al., 2012). Another study supports the ability of MALDI-TOF MS to detect the activity of carbapenemase of enteric bacteria and pseudomonas (Croxatto et al., 2012a).

Application of MALDI-TOF in virology is quite distinct from the work in bacteriology. The analysis is of samples is challenging due to low protein expression in most of the viruses. PCR amplification is often required before MALDI-TOF analysis for viruses (Sjöholm et al., 2008). In mycology, the ascomycetous and basidiomycetous yeasts have been reported to have high quality of PMF profiles, while other families of fungi are still difficult to extract due it their biological complexity and co-existence with different fungal phenotypes. Thus, MALDI-TOF may not be the best option for fungal identification (Santos et al., 2010).

1.4.2 Fourier Transform -Infrared Spectroscopy (FT-IR)

Fourier Transform-Infrared Spectroscopy is another emerging technology that could provide a fast method to identify microorganisms. Similar to MALDI-TOF MS, FT-IR produces spectral fingerprints that are unique for various species of bacterial strains. The basis of FT-IR analysis is on the measurement of infrared region of the electromagnetic radiation spectra. IR spectra are formed due to the absorption of energy released by the molecular bond that undergoes vibrational excitation. Each molecule, like proteins in the sample, has different bonds that absorb energy at different frequencies. Hence, it should be expected that the patterns of various bacterial species must be distinct (Rodriguez-Saona et al., 2001). A technique called attenuated total reflectance (ATR) is integrated into FT-IR system. ATR technique enables the instrument to collect IR radiation reflected from the surface of viscous and thick samples (Ojeda & Dittrich, 2012).

Bruker Daltonik developed FT-IR Biotyper (Biotyper-IR) specific for bacterial identification with a spectroscopy system focusing on the vibration of carbohydrate constituents such as glycoproteins (Rodriguez-Saona et al., 2001). The bacterial cell surface is the key analyte, which allows FT-IR to detect and differentiate various bacterial species. For example, the cell surface between Gram-negative and Gram-positive bacteria are distinct from each other. Gram-negatives have a low amount of peptidoglycan and a high amount of lipopolysaccharides (LPS), whereas Gram-positive bacteria are composed of mostly peptidoglycan with lipoteichoic acids. Some bacteria might have capsules, flagella, fimbriae, glycolates, lectins, and mycolic acids—all of these distinct properties of cell surface produce wide variety of IR spectra. Thus, comparison of two IR spectra from different organisms could be performed easily (Rodriguez-Saona et al., 2001).

The sample preparation for FT-IR varies depending on the bacterial species. For mycobacteria, Scheer *et al.* suspended a liquid colony of mycobacteria, pre-treated it with warm water, and diluted the sample before inoculating it in the agar plate. This method produces a consistent amount of colony to produce good quality IR spectral (Rebuffo Scheer et al.,2017). Bosch *et al.* prepared sample for Gram-negative bacteria by harvesting a loopful of sample and suspending it with distilled water. Afterwards, he aliquoted the bacterial suspension in the optical plates and left it to dry. The formation of thin bacterial film could be seen from the plates (Bosch et al., 2008).

There are several types of analysis used for FT-IR. Analysis such as Principle Component Analysis (PCA) and Soft Independent Modeling of Class Analogy (SIMCA) are commonly used for bacterial identification. The basic theory of FT-IR is based on the absorbance of the functional group present in the samples. The absorbance values will then be calculated by PCA

or SIMCA algorithm. PCA directs data into linearly uncorrelated variables and organizes the data based on variance within the data. SIMCA utilizes a distinct PCA model for each class of variables.

Since FT-IR is quite new technology, the evaluation and application of this technology is still limited to some bacterial species such *as Enterobacteriaceae, Staphylococcus, Aeromonas, Pseudomonas,* and *Cyanobacteria*. FT-IR can discriminate different bacteria taxa down to the strain level (Rodriguez-Saona et al., 2001). The application of FT-IR in virology is possible for detection and viral quantification. Montiel *et al.* grew cell culture as biosensor in the ZnSe crystal, and he transfected the poliovirus in the cell culture for FT-IR analysis. Non-infected and infected cells produced distinct IR profiles (Lee-Montiel et al., 2011). FT-IR can also characterize fungi from food spoilage down to species level (V Shapaval et al., 2013). Furthermore, Grunert *et al.* attempted to serotype the capsule of *S. aureus* with FT-IR assisted artificial neural networks (ANN) analysis. Both external and internal validations of *S. aureus* capsular typing value show promising results of 96.7% and 98.2% (Grunert et al., 2013).

1.4.3 Serological Tests

Detection for MAC, particularly MAP, could be done indirectly by enzyme-linked immunosorbent assay (ELISA). As it is mentioned before, the infection of MAP induces T-helper cells to produce IFN-γ. The changes in IFN-γ level can be measured in an ELISA. In this study, one day old blood culture supernatants are taken from cattle that has been stimulated with Johnin—a purified protein derivatives from MAP—and bovine IL-12 (Jungersen et al., 2012). However, this test is not effective as it is reported there is cross-reactivity between Johnin protein and IFN-γ. Another alternative could be using lipopeptide L5P, which is the cell wall of MAP. A

study used this antigen for the ELISA assay, but the results showed lower value as compared to the one with Johnin proteins (Jungersen et al., 2012) .

1.4.4 Real Time PCR

The most common diagnostic test with PCR uses IS900 as the target, but as mentioned before, this target gives false positive results (Erume et al., 2001). New target sequences specific for MAP have been identified. Sequences such as ISMAP02 present in MAP in multiple copies. This target combined with IS900 could improve real time PCR sensitivity (Park et al., 2016). A study from Shin et al. with five targeted multiplex PCR could significantly detect different members of MAC. A chromosomal target DT1, which is specific for MAA, MAS, and MAI along with IS900, IS901, and IS1311 are the targets for multiplex PCR. 53 MAC reference strains consisting of 28 different mycobacteria strains were tested to evaluate the identification accuracy for this method. There was 100% agreement between MAC multiplex with isolates. Hence, this novel method could be one of best potential for MAC detection and identification (Shin et al., 2010).

2. Matrix Assisted Laser Desorption/Ionization Time-of-Flight Mass Spectrometry (MALDI-TOF) Project

2.1 Introduction

Over the past few decades, infections due *Mycobacterium avium* complex (MAC) have become a major problem in livestock industries and contribute to large economic losses and morbidity of livestock. Two clinically important subspecies of *M. avium* are *M. avium* subsp *paratuberculosis* (MAP) and *M. avium* subsp *hominissuis* (MAH). MAP is the etiologic agent of Johne's disease, a chronic and fatal enteritis in ruminants that has been linked to Crohn's disease in humans. MAH has zoonotic potential as it is one of the leading causes of secondary infections

in AIDS patients. Identification of M. *avium* subspecies is still challenging because the strains have overlapping host ranges and clinical signs. Information about the host specificity of *M. avium* also has not been determined. Therefore, tracing the infection sources to reduce the transmission is difficult. Currently, common diagnostic tests for *M. avium,* such as blood and biochemical tests, are labor intensive, time consuming, and, in certain cases, unreliable. Advanced diagnostic tools, namely matrix-assisted laser desorption ionization time-of-flight mass spectrometry (MALDI-TOF MS), could provide a rapid, low-cost, and accurate diagnostic test to differentiate MAP. This test could be implemented into diagnostic workflows in veterinary diagnostic labs, where this technology is often already in use. The purpose of this project is to differentiate *M. avium* subspecies from field isolates (particularly MAP and MAH), distinguish these isolates from other members of the *M. avium* complex (MAC), and determine the host species of origin using MALDI TOF MS library and biomarker based proteomic approaches.

2.2 Materials and Methods

Bacterial strains: A total of 57 bacterial isolates that include 33 MAP isolates, 22 non-MAP isolates, and 2 ATCC references strains were used in this project. The field isolates were previously identified with morphological and genomic approaches by PCR at Dr.Collins' lab at UW-Madison, Dr.Barletta's lab at UNL, or were acquired from ATCC. The species of the isolates comprised of *M. avium ssp paratuberculosis, M avium ssp hominisuis, M.intracellulare, M avium ssp avium, M avium ssp silvaticum,* and non-tuberculous mycobacteria. All the strains were isolated from various hosts from different states within the United States.

MALDI-TOF Sample Preparation: After preliminary work examining different extraction protocols, the heat inactivation and extraction method for *Mycobacteria sp* recommended by the

manufacturer was utilized in this project. Biomass of mycobacteria was collected (approximately one to two 10µL inoculation loops) from solid media and suspended in 300µL deionized water. Heat inactivation was accomplished in the thermoblock with 98°C temperature, followed 900µL EtOH addition, and centrifuged for 2 minutes. The supernatant was removed completely, and the pelleted cells were resuspended in 500 µL deionized water and centrifuged. Next, the cell lysates were subjected to formic acid and acetonitrile extraction procedures and vortexing. In addition, to break the cell wall of mycobacteria, the bead beating using 0.5 mm zirconia-silica bead were applied (during vortexing) to get the intracellular protein of the cells. The extracted samples were spotted each 1 µL on the MALDI target plate together with HCCA matrix (a-cyano-4-hydroxycinnamic acid) and incubated to dry. Analysis process to generate spectral profiles were done by manufacturer's software (Bruker Biotyper).

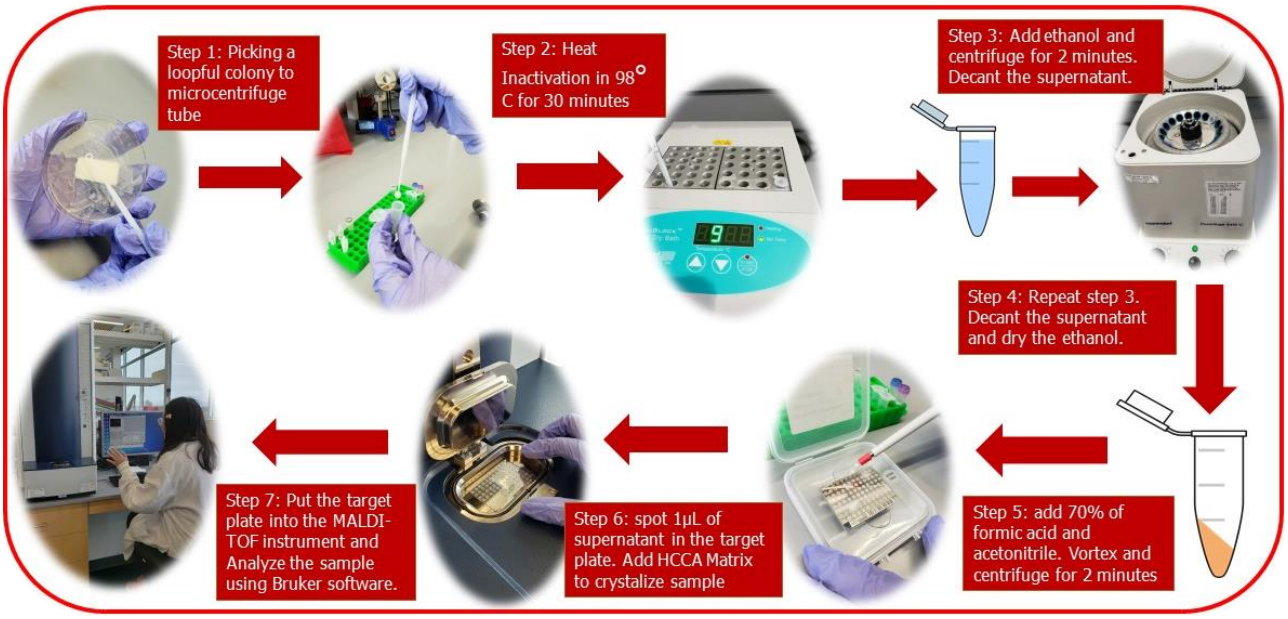

Figure 1: The Schematic of MALDI-TOF Heat Inactivation Methods

2.3 Results

MALDI-TOF MS Analysis: fourty-seven out of 57 isolates were able to generate valid spectral profiles. Comparative evaluation between these isolates and reference spectral profiles from Bruker Daltonics (BDAL) database exhibited average log score values of <2.0 as shown in the *Table 1*. Only 14 isolates had log score values higher or equal to 1.6, which is the minimum standard value for identification. Thus, the BDAL database only can appropriately classify 29 % (14/47) of *M. avium*. In contrast, most of the isolates that were matched against the custom main consensus library (MSP) generated from *M. avium* isolates displayed a much higher log score with values of >2.0. This new library could accurately identify 85% (40/47) of *M. avium* at the species level, which significantly improved identification accuracy. Furthermore, MALDI-TOF MS was able to characterize *M. avium* at subspecies level as it is shown in *Figure 1*. The dendrogram shows clusters of non-MAP strains and MAP strains that agree with the PCR results from Dr.Collins' lab. In *Figure 4*, two major clusters of MAP were identified. The bottom cluster of MAP is more closely related to MAH, while the top cluster of MAP does not have relation to MAH. Non-tuberculous mycobacteria and *M. intracellulare* have the furthest distance, which corresponds to less overall genetic relatedness to MAP as both are not a member of *M. avium*. Interestingly, two reference strains, *M. avium silvaticum* (ATCC 49884) and *M. avium avium* (ATCC 25291), do not cluster together although both strains have similar host ranges in avian and pigeon.

MALDI-TOF Kappa Analysis: Cohen's Kappa Analysis was calculated using JMP 15 Pro (SAS Institute Cary, NC) software to verify the agreement (K value) between top match score subspecies and the multiplex PCR-ID subspecies in *Table 1*. If the top match score subspecies was similar to the subspecies from PCR-ID and the score was above 2, it was indicated as "1" or

agreement in the Kappa analysis, and "0" if it does not match or had lower values. There were 6/45 isolates having "0" Kappa analysis and the rest of the isolates (39/45) indicating "1" Kappa analysis. The K-value for the MSP database was found to be 0.73, portraying overall "good" levels of agreement (*Table 2 and 3).*

2.4 Discussion

Prevention and early diagnosis of MAP is critical since it causes significant economic lost in the dairy industry, along with its correlation to Crohn's Disease in humans. Tracing and characterizing the sources of the disease with a rapid, high accuracy instrument would be beneficial over traditional methods. Multiplex PCR method remain the "gold standard" for molecular typing down to subspecies level, even though it has several drawbacks, such relative high cost, labor intensive, and time consuming. This may not be advantageous in clinical lab settings. Furthermore, the multiplex PCR methods require primers designed to target sequences specific to the subspecies for DNA amplification in the PCR. The method is more complicated for the present application since subspecies members of MAC have multiple unique target sequences. For instance, in *M. avium ssp avium*, specific probes must be made to target chromosomes, named DT1. Moreover, two others in MAC—*M. avium silvaticum* and *M. intracellulare* –need three probes to target insertion sequences of IS 900, IS 901, IS 1311(Mijs et al., 2002). The research described here and from the aforementioned study suggest MALDI-TOF could be a potential tool for rapid diagnosis of MAP in the clinical setting(Croxatto et al., 2012a). By creating MSP for all members of MAC, the accuracy of MALDI-TOF to identify subspecies of MAP could improve further. *Figure 2 and 3* portray comparison between top match scores of BDAL and MSP. The BDAL provides lower value (1.45) than the MSP (2.7). BDAL database collections are comprised of various isolates of bacterial species, which is not

specific for MAP. There are only four mycobacteria fingerprints in this database and only one being MAP (ATCC 19698). This could be the reason BDAL provides a lower top match score, as the software algorithm could not recognize a similar pattern to the one MAP representative, indicating a higher level of strain diversity that is not represented in the current database. The new MSP database provides a fingerprint collection specific for MAC members. Thus, the algorithm could detect the MAP fingerprint pattern more accurately. For MAP isolates, the BDAL database could only give an 18% level of good match scores in total, while the MSP provided 93%. This indicates a 75% increase in matching accuracy. For non-MAP, the matching accuracy only enhances 47%. It remains unclear what factors are involved in reduced matching accuracy for non-MAP, but contaminated samples could be one factor, as we did not administer antibiotic in the 7H9 media. It has been observed that non-MAP can be easily contaminated with other bacterial species because its colony morphology could be similar to commensals, having slimy and wetter colonies than MAP. Overall, since the Kappa analysis yield good agreement after the creation of new MSP, the application of MAP diagnosis with MALDI-TOF is possible as an alternative over PCR methods.

Despite the advantages of MALDI-TOF for MAP diagnosis, the limitations are in the sample preparation. It requires long incubation time to grow both non-MAP and MAP. Non-MAP requires almost one-week incubation, while MAP takes three weeks to four weeks. Cell extraction for MAP is complex and it is time consuming some for vortexing with zirconia silica beads. The concentration of formic acid and acetonitrile could affect the extraction process. Better spectral profiles are generated when cell lysates are more concentrated with these reagents. Yet, reducing the amount of reagent could increase noise and result in insufficient cell lysates for replicates. Some studies suggested the quality of spectral profiles depends on the

sample preparation. Thus, sample with some unextracted cells or non-homogenized cells could result in distinct spectral profiles. During this research process, some MAP isolates were difficult to grow and had a lot of noise signal. Second attempts to extract these MAP isolates were done, but the cell lysates could not be processed homogenously due to the dry and waxy nature of the MAP colonies. This has complicated the result in the dendrogram shown in the *Figure 4*. We expected that there would only be two large clusters of MAP and non-MAP. However, it displays otherwise in *Figure 4.*

The result of dendrogram *(Figure 4),* displays interesting potential relationships between members of MAC. *M. intracellulare* and non-mycobacteria were expected to have their own cluster since they are phylogenetically distinct from other subspecies of MAC (shown in the phylogenetic figure). Both *M. avium silvaticum* and *M. avium avium* are known to predominate birds, yet in the dendrogram, *M. avium avium* is more closely related to *M. hominissuis* than to *M. silvaticum.* Apparently, *M. hominissuis* was named after *M. avium avium* which had adapted to mammalian hosts. Thus, they have shorter genetic distance (Mijs et al., 2002).

2.5 Conclusion

To conclude, MALDI-TOF MS could be a good alternative tool for a diagnostic test to rapidly characterize and identify *M. avium*. The new library database that was created in this project could significantly enhance the sensitivity of the instrument as it increases the matching score values using well characterized isolates. Over 85% of the isolates could be classified correctly using our new MSP database, whereas the current BDAL database could only characterize the isolates in 29% of cases. Although there were seven isolates that failed to have a higher score value when using our MSP database, their top match values were still greater as compared to the BDAL database score. Therefore, we consider that our new MSP database is a

large improvement over the previous database. Our MSP dendrogram (*Figure 4* exhibited accurate characterization, which shows a potential that MALDI-TOF could discriminate *M. avium* complex (MAC) down to subspecies level. Each strain forms clades corresponding to their subspecies. For determining host specificity, our results need to be further investigated as we did not see a host-range relationship. However, it is interesting that there are two MAP clusters that separate from each other as well as MAH. Other approaches using bioinformatics analysis to look at specific peaks within spectra (Clinpro tools) and Fourier-Transformed infrared spectrometry (FT-IR) may be administered for further research of this topic to evaluate host specificity amongst MAP strains. Overall, as we enhance the breadth and quality of MALDI-TOF MS database, we demonstrated that a rapid diagnostic test for identification of *M. avium* is possible, and thus provide new tools to enable enhanced detection and mitigation of MAP on farms.

2.6 List of Tables and Figures

Table 1

Comparison of multiplex PCR-ID to MALDI-TOF database (BDAL) and custom database MSP top match score, for differentiation of MAP and non-MAP.

Isolate ID	**State**	**Isolate Sources**	**Top Match Score BDAL♦**	**Top Match Score MSP∆**	**PCR ID**	**Group**
JTC 1536	Florida	Waterbuck	1.32	1.98	*M. Intracellulare*	Non MAP
JTC 1537	Florida	Impala	1.27	1.27	*Non-Mycobacteria*	Non MAP
JTC 1538	California	Formosan Muntjac	1.31	2.57	*M. avium hominissuis*	Non MAP
JTC 1539	California	Blesbok	1.31	2.59	*M. avium hominissuis*	Non MAP
JTC 1540	California	Ellipsen Waterbuck	1.85	2.44	*M. avium hominissuis*	Non MAP
JTC 1542	California	Addra Gazelle	1.10	2.31	*M. Intracellulare*	Non MAP

JTC 1543	California	Mule Deer	1.79	2.21	*M. avium hominissuis*	Non MAP
JTC 1544	California	Burmese Thamin	1.22	2.38	*M. Intracellulare*	Non MAP
JTC 1546	Minnesota	Pygymy Goat	1.16	1.9	*M. Intracellulare*	Non MAP
JTC 1547	Minnesota	Elk	1.25	2.17	*M. avium hominissuis*	Non MAP
JTC 1548	Wisconsin	Pygymy Goat	1.63	2.09	*M. avium hominissuis*	Non MAP
JTC 1549	Montana	Bison	1.18	2.36	*M. Intracellulare*	Non MAP
JTC 1550	Montana	Bison	1.64	2.44	*M. avium hominissuis*	Non MAP
JTC 1551	California	Waterbuck	1.35	2.23	*M. avium hominissuis*	Non MAP
JTC 1552	Montana	Bison	1.94	2.4	*M. avium hominissuis*	Non MAP
ATCC 49884	ATCC	-	1.26	1.99	*M. avium silvaticum*	Non MAP
ATCC 25291	ATCC	-	1.58	1.93	*M.avium avium*	Non-MAP
DT 267	Minnesota	Pygymy Goat	1.44	2.55	*M.avium paratuberculosis*	MAP
DT 268	Minnesota	Pygymy Goat	1.66	2.53	*M.avium paratuberculosis*	MAP
DT 269	Minnesota	Pygymy Goat	1.65	2.70	*M.avium paratuberculosis*	MAP
DT 3	California	British Red Deer	1.37	2.41	*M.avium paratuberculosis*	MAP
DT 590	New York	Gibbon	1.24	2.52	*M.avium paratuberculosis*	MAP
DT 639	Montana	Bison	1.56	2.62	*M.avium paratuberculosis*	MAP
DT 738	California	Tule Elk	1.8	2.73	*M.avium paratuberculosis*	MAP
DT 774	California	Tule Elk	1.24	2.65	*M.avium paratuberculosis*	MAP
JTC 1094	Wisconsin	Nubian Goat	1.32	2.57	*M.avium paratuberculosis*	MAP
DT 812	Montana	Elk	1.42	2.60	*M.avium paratuberculosis*	MAP
JTC 1180	Florida	Key Deer	1.57	2.45	*M.avium paratuberculosis*	MAP
JTC 1533	Barletta's lab	-	1.23	2.56	*M.avium paratuberculosis*	MAP
JTC 1250	California	Hog Deer	1.43	2.7	*M.avium paratuberculosis*	MAP
JTC 1344	Florida	Key Deer	1.77	2.6	*M.avium paratuberculosis*	MAP

JTC 1353	Florida	Key Deer	1.2	2.56	*M.avium paratuberculosis*	MAP
JTC 1386	Florida	Key Deer	1.38	2.73	*M.avium paratuberculosis*	MAP
JTC 1528	California	Tule Elk	1.21	2.39	*M.avium paratuberculosis*	MAP
JTC 1529	California	Tule Elk	1.44	2.61	*M.avium paratuberculosis*	MAP
JTC 1527	California	Tule Elk	1.6	2.67	*M.avium paratuberculosis*	MAP
JTC 1531	California	Tule Elk	1.32	0.73	*M.avium paratuberculosis*	MAP
JTC 1532	Minnesota	Pot-Bellied Pig	1.48	2.65	*M.avium paratuberculosis*	MAP
JTC 1534	Barletta's lab	-	1.52	2.57	*M.avium paratuberculosis*	MAP
DT 775	California	Tule Elk	1.21	2.29	*M.avium paratuberculosis*	MAP
JTC 932	Michigan	Bison	1.34	2.52	*M.avium paratuberculosis*	MAP
JTC 1005	Wisconsin	Bovine	1.67	2.07	*M.avium paratuberculosis*	MAP
W244	Wisconsin	Bovine	1.58	1.66	*M.avium paratuberculosis*	MAP
DT 864	Wisconsin	Bison	1.98	2.57	*M.avium paratuberculosis*	MAP

♦ BDAL = Bruker Daltonics (Manufacturer database). Indicates top match scores from manufacturer database.
Δ MSP= customized consensus main spectrum. Indicates top match scores from the customized database.

Agreement Statistic

Kappa Coefficient

Degree of Agreement	Kappa	Std Err	Lower 95%	Upper 95%
	0.739693	0.077048	0.588682	0.890704

Table 2: Kappa analysis between PCR and MSP database has value of 0.739, indicating a good agreement.

Kappa Analysis

Value of K	Strength of Agreement
<0.20	Poor
0.21 – 0.40	Fair
0.41 – 0.60	Moderate
0.61 – 0.80	Good
0.81 – 1.00	Very Good

Table 3: Kappa Analysis table, indicating strength of agreement as poor, fair, moderate, or good.

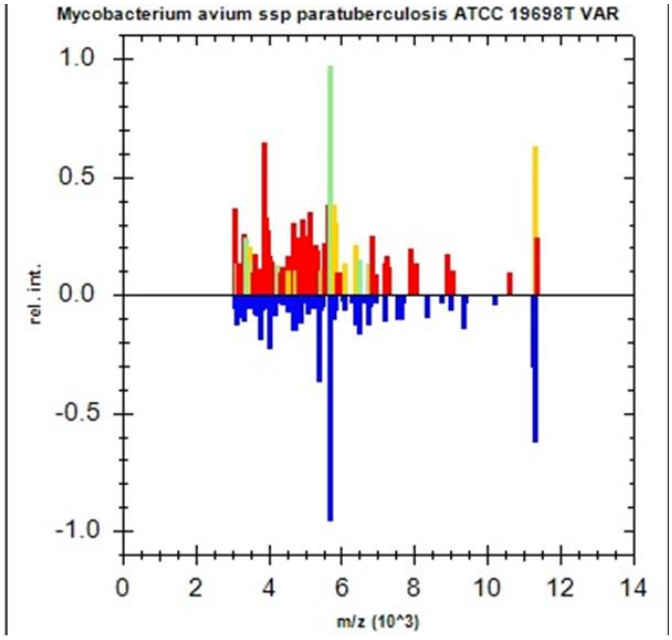

Mo	Detected Species	Log(Score)
	Mycobacterium avium ssp paratuberculosis JTC 1386	3.000
	Mycobacterium avium ssp paratuberculosis ATCC 19698T V...	1.450
	Mycobacterium avium 08 TWF	1.440
	Mycobacterium avium TB RV422 4 02 UKE	1.380
	Lactobacillus pentosus DSM 20199 DSM	1.290
	Mycobacterium bovis Bovinus An 1 PGM	1.260
	Streptomyces violaceoruber B263 UFL	1.260
	Candida parapsilosis ATCC 22019 THL	1.260
	Rhizobium radiobacter B166 UFL	1.220
	Aromatoleum alkani HxN1 MPB	1.200

Figure 2: Mass spectrum output (Upper Panel) shows MAP JTC 1386 fingerprints compared to isolates ATCC 19698 from BDAL database. Green peaks represent strong matches, yellow are intermediate matches, and red are mismatches. The bottom table displays the top match log score between both isolates is 1.45.

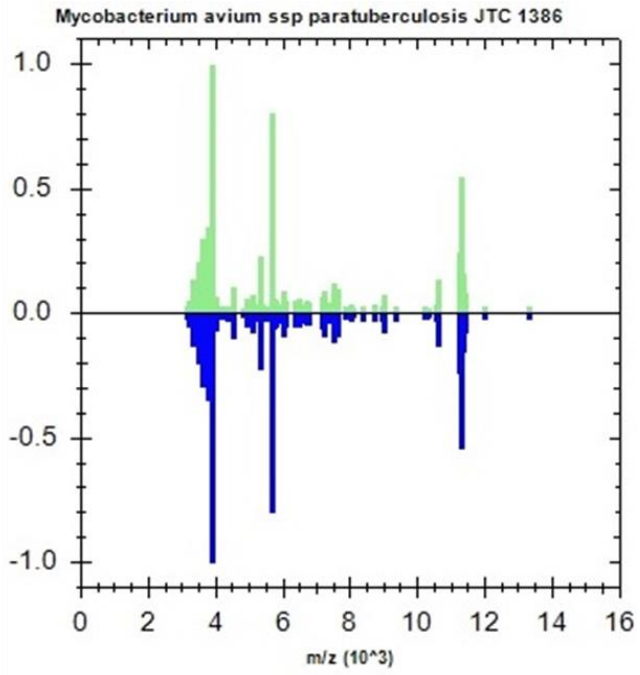

Mo	Detected Species	Log(Score)
	Mycobacterium avium ssp paratuberculosis JTC 1386	3.000
	Mycobacterium avium ssp paratuberculosis DT 738	2.730
	Mycobacterium avium ssp paratuberculosis DT 269	2.710
	Mycobacterium avium ssp paratuberculosis JTC 1250	2.690
	Mycobacterium avium ssp paratuberculosis JTC 1527	2.670
	Mycobacterium avium ssp paratuberculosis DT 639	2.620
	Mycobacterium avium ssp paratuberculosis JTC 1386	2.260
	Mycobacterium avium ssp paratuberculosis JTC 1344	2.200
	Mycobacterium avium ssp paratuberculosis DT 864	2.150
	Mycobacterium avium hominissuis JTC 1552	2.130

Figure 3: comparison between MAP JTC 1386 and consensus main spectrum (MSP) of all *M.avium* complex isolates. The new MSP database has top matches log score of 2.73, which is significantly improved than the BDAL database on the left.

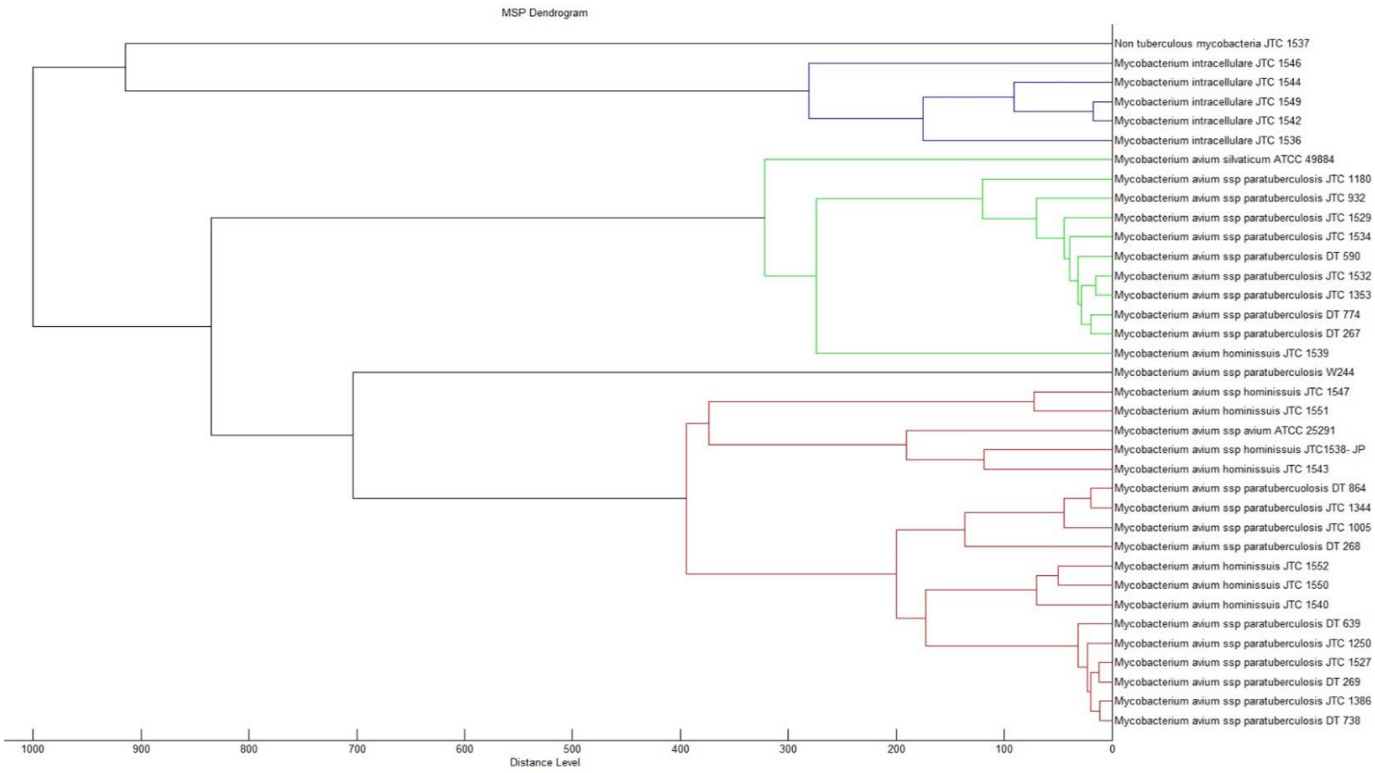

Figure 4: Dendrogram generated from a consensus main spectrum (MSP) of *M. avium* isolates shows clustering at species and subspecies level. Note that there are two clusters of MAP, two clusters of MAH, and two reference strains and one non tuberculous strain that does not cluster. The dendrogram displays distance based average relation algorithm normalized to an arbitrary distance of 1000

	# Isolate Tested	BDAL Database	MSP Database
MAP	28	5/ 28 (18%)	26/28 (93%)
Non-MAP	17	4/ 17 (24 %)	12/17 (71%)
Total	45	9/45 (20 %)	38/45 (84%)

Table 4: New MSP library database significantly improves identification accuracy for 64% as compared to BDAL database.

3. Fourier-Transform Infrared Spectroscopy Project

3.1 Introduction

Previously, MALDI-TOF MS based methods were developed that enabled differentiation within subspecies of MAP. However, it still was unable to trace the host species of origin, which is critical for prevention of MAP transmission in herds. The pathogenicity and virulence of MAP towards specific hosts has not been determined, yet some MAP strains often have host preference. MAP strain type C dominates infection in cattle, type S in sheep, and type B in bison. This classification only partially reflects their host-specificity, being the types named after the host from which they were originally isolated. Some cases have demonstrated that the strains can have overlap in host range, and they may have altered or no clinical signs in other hosts. Thus, early diagnostic tests to distinguish those types of MAP are required to find the host origin, reduce livestock morbidity, and to assess potential clinical significance. An advanced diagnostic tool, Fourier Transformed Infrared Spectroscopy (FT-IR), is one potential approach for precise characterization of MAP types. The instrument is able to generate a distinct infrared fingerprint spectrum that could potentially discriminate various types of MAP by absorbing infrared radiation of specific MAP mycolic-acid rich regions. Furthermore, a previous study has proven that FT-IR is able to differentiate various strains of *M. fortuitum*, and it facilitates classification of microbial multispecies populations (Rebuffo Scheer et al.,2017). However, there is no information on the evaluation of this technology looking at the strain level of MAP, including its host type. Hence, our goal was to look for specific cell surface biomarkers that characterize the host types of MAP based on the IR spectral fingerprints and to arrange a hierarchical cluster agreement (HCA) portraying the clustering of isolated strains. Genome information indicates C, S and B type strains of MAP are distinct. This means that the molecular composition of each

type of MAP likely differs, particularly the mycolic-acid region (Bryant et al.,2016). We hypothesized that FT-IR will allow differentiation of MAP strains based on the host range (C, S, and B type)

3.2 Materials and Methods

Bacterial strains: A total of 57 bacterial isolates that include 33 MAP isolates, 22 non-MAP isolates, and 2 ATCC references strains were used in this project. The field isolates were previously identified with morphologic and genomic approaches by PCR at Dr.Collins' lab at UW-Madison and ATCC. The species of the isolates comprised of *M. avium* complex members: *M. avium ssp paratuberculosis, M. avium ssp hominisuis, M. intracellulare, M. avium ssp avium, M. avium ssp silvaticum,* and non-tuberculous mycobacteria. The strains were isolated from different states with broad host ranges such as bison, cattle, elk, pig, deer, goat, gibbon, waterbuck, blesbok, and thamins.

FT-IR Sample Preparation: The method for this research project was developed independently in Dr. Loy's lab using multiple dilution factors. The bacterial isolates were grown at 37°C in the liquid media Middlebrook 7H9 supplemented with OADC and ferric-mycobactin J. Upon 2-3 weeks growth (depending on the strain), the cultures were centrifuged for 15 minutes at 2500 rpm and the supernatant discarded. The pellet was suspended in 70% (v/v) ethanol and water, then the sample was transferred to the suspension vials containing metal bars. For each dilution factor, the cells were homogenized by vortexing and pipetting up and down. Six replicates with different dilution factors were made for each individual strain. Next, the homogenized samples were spotted on the FT-IR target plate and incubated at 37℃ for 5 minutes. The spectral analysis was carried out using an IR Biotyper System (Bruker Daltonik,

Bremen, Germany) and Opus Software with the default analysis settings as recommended by the manufacturer.

3.3 Results

MAC Infrared Spectra

Figure 5 displays infrared spectra profiles of five different strains of *M. avium* complex (MAC) and one non-mycobacteria (*Moraxella bovoculli*). All strains had intense bands in the 3300 cm^{-1} region. Two strong bands located in the 2800 and 3000 cm^{-1} regions presented in five strains of MAC spectra, while the non-related strain *Moraxella* did not. No major differences were observed between five strains of MAC. However, *M. avium avium* and *M. avium hominisuis* seemed to have a unique peak present in the 1750 cm^{-1} region and one small peak at 3000 cm^{-1}.

Host Species of MAC

There was no relevant group of host species of origin present in the non-MAP hierarchical cluster analysis (HCA) as in *Figure 6*. Nevertheless, analysis based on the isolates location *(Table 1)* showed strains (JTC 1551, JTC1538, JTC 1541) and (JTC 1540 and JTC 1543) from California formed groups. The optimal cut off for this dendrogram was the lowest *(Figure 6)* having value of 0.002, and most isolates have cluster purity colored orange indicating "medium". The cut-off value refers to their genetic distance. Small cut off values indicates close relation between strains. *Figure 7* portrays HCA of MAP host species of origin. Some isolates from similar hosts do cluster together. One cluster comprising JTC 1344, JTC 1180, and JTC 1341 belong to the same host of key deer. Similarly, DT 774 and 775 from Tule Elk clustered together. The optimal cut-off is 0.09 varying cluster purity from medium (orange), bad (yellow), and good (green). There was no clustering based on location observed in MAP dendrogram.

Differentiation of MAP and Non-MAP

The collection of MAP and non-MAP IR spectra were compiled together generating the dendrogram in *Figure 8*. The optimal cut off for this dendrogram was the highest (0.12) and the cluster of all MAP isolates were "good", but the non-MAP isolates were "medium". Two big clusters of MAP were observed, one on the top and the bottom. One cluster of non-MAP was present, but there was an outlier of *M. silvaticum*. *Figure 6* depicts characterization of non-MAP. There was no significant grouping found.

3.4 Discussion

Characteristics of MAC IR Spectra

The spectra of FT-IR possess unique and distinct characteristics from MALDI-TOF spectra. Infrared spectra are measured based on the energy absorbed due to breaking bonds of functional groups in the cell surface components (Davis & Mauer, 2010). Different bacterial species have complex cell surface components, enabling production of distinct IR fingerprints for each species. As any other mycobacteria, specific components of MAC will be in their mycolic acid-rich cell wall (Chatterjee, 1997). The composition of mycolic acid is abundant with fatty acid (Volha Shapaval et al.,2019). The stretching of fatty acid bonds will appear in the region 2800 cm^{-1} to 3000 cm^{-1} (Volha Shapaval et al., 2019)as is shown in *Figure 5* of the five strains of MAC. The 3300 cm^{-1} region signifies amide bonds stretching in the nucleic acid, hence all the bacterial isolates must have intense peak in this region. As MAC is Gram-positive, there should be no band observed in the 1200 cm^{-1} region, as this indicates the presence of polysaccharides. On the other hand, *Moraxella bovoculi*, which is a Gram-negative, is lacking the peak in this region. *M. bovoculli* has been known to have high genetic diversity and distinct virulence factors, especially in the capsular polysaccharide (Dickey et al., 2018). This could indicate that the *M.*

bovoculli IR spectra in *Figure 5* may not have a high amount of polysaccharide. The strong band in the 1750 cm^{-1} region demonstrates the presence of amide bonds in the peptide. This signature is specific to *M. avium avium* and *M. avium hominisuis*. It is unclear what type of protein is indicated by this band, but a study revealed that *M. avium hominisuis* emerged from *M.avium avium* after adaptation to mammals(Mijs et al., 2002). Supporting this concept of relatedness, both strains had a small peak at 3000 cm^{-1}.

Host Species of Origin of MAC

Although a study (Alonso-Hearn et al., 2017)of fatty acid profiling reveals changes in MAP cell structure after infection in the host macrophage, the results summarized in *Figure 7 and 8* do not reflect the IR capability to find the differences. The pattern of the mycolic acid region in 2800 to 3000 cm^{-1}*(Figure 5)* between strains of MAC may look slightly different, but this change is insignificant and there is no standard pattern that signifies the changes of the different host species of origin. The fact that *Figure 7* has two host species of origin clusters implies that MAP may undergo more host-adaptation changes than non-MAP species. For bacteria to evolve, cell division time and the host environment are the biggest factors. Hence, in *Figure 7*, some MAP isolates that are not clustering may not have sufficient factors to undergo adaptation in their new hosts.

Differentiation of MAP and Non-MAP

FT-IR could be a better instrument than MALDI-TOF for bacterial differentiation because the IR spectra generated provide specific signature bands from each bacterial species that are present on the cell membrane. MALDI-TOF spectra works by matching the peptide fingerprints generated from intracellular proteins and enable comparison between the database and isolates (Croxatto et al., 2012b), but the peaks in the fingerprints are not signify the chemical

molecules present in the bacterial cell. Thus, analysis for distinct bacterial species will be easier with the IR spectra on the basis of the cell membrane composition. The *Figure 5* dendrogram shows very clear differentiation of MAP and non-MAP, and *Figure 5* is also similar to MSP dendrogram in *Figure 4 (2.6)*. Two clusters of MAP emerge with one closely related to the non-MAP and the other has farther distance. The optimal cut off point is the highest for *Figure 8*, representing best clustering. Non-MAP subspecies can also cluster together as shown in *Figure 9*, but there is no relevant explanation pertaining the relative closeness between subspecies since there were no major similar IR spectra found. As in *Figure 5*, *M. avium silvaticum* possessed band patterns similar to that *M. intracellulare* and MAP. This may explain their subspecies correlation, although this fact is still inconclusive because the band patterns are distinct for each replicate from the same isolates. The major disadvantages of FT-IR are similar to MALDI-TOF, which is in the sample requirements and preparation. Depending on the characteristics of each MAC colony, the treatment, dilution factor, and band pattern emitted will be diverse for each sample. This makes analysis of the IR spectra more challenging. Work has been done in this project using a spectrophotometer to allocate the same optimum optical density for each sample. Nevertheless, there was no good standard of OD observed for each isolate, and it was also dependent on the colony morphology. Some colonies are wetter have more cells; hence, when such a colony is taken in one full inoculation loop, it creates too much noise. On the other hand, the waxy and dry colonies have fewer cells; thus, more than one full inoculation loop is needed and extra time for vortexing to get high quality IR spectra.

3.5 Conclusion

In general, both MALDI-TOF and FT-IR are promising instruments for quick and fast detection and identification of MAC. Precise characterization of non-MAP and MAP is also

possible using these two instruments. However, FT-IR more useful than MALDI-TOF for spectra analysis. Researchers could easily detect the signature band pattern on the basis of bacterial cell wall composition, providing enhanced certainty of sample identification. Besides that, the HCA dendrogram could be customized to diverse categories within one spectral collection. As for tracking the host species of origin of MAC, the result is still indecisive because the HCA results are not consistent. However, there may be application for this technology regarding host-origin for other bacterial species that undergo quick host-adaptation and have external cell structure such as capsule. Host species of origin in MAP could be partially identified as in *Figure 7*. Possibly, these isolates have adapted to their host and change their bacterial components, whereas other MAP isolates that are not clustering are still undergoing slow adaptation in the host with less change. Since non-MAP are mostly present in wildlife, there is less evidence showing their adaptation to specific hosts. They could become opportunistic pathogens to any hosts. For instance, *M. avium avium,* which is naturally found in the avian group could cross infect porcine for an indefinite time of evolution until it was tested to have a distinct genome and subdivided to be M. *avium hominissuis* (Mijs et al., 2002). Hence, *Figure 6* is consistent with this study. The overall optimal cut-off for MAC is relatively low because of their complex bacterial structure and colony morphology, in addition to inequivalent sample preparation treatment (e.g different dilution factor and timing of vortexing). Obtaining good spectra remains the most challenging aspects for both MALDI-TOF and FT-IR instrument. The slow growth of MAC impedes the ability for rapid identification of MAC in the clinical lab, but the technology procedures are faster and cheaper as compared to other serological or multiplex PCR testing (Shin et al., 2010).

3.6 List of Tables and Figures

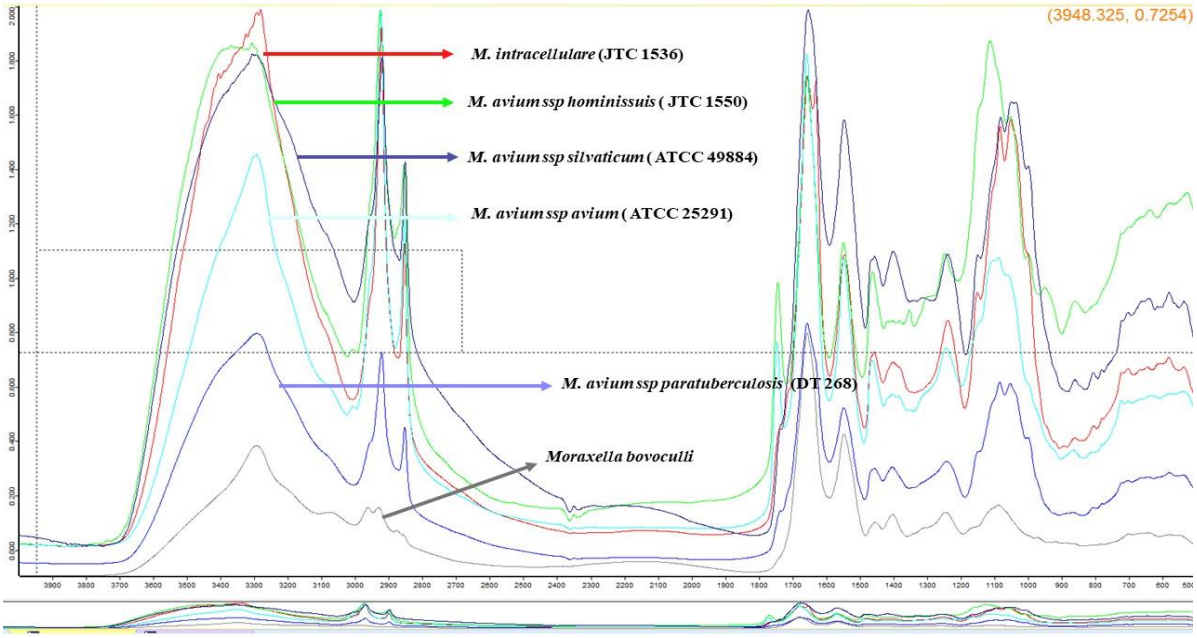

Figure 5: IR spectra profiles of five strains of MAC and one non-related strain of Moraxella.

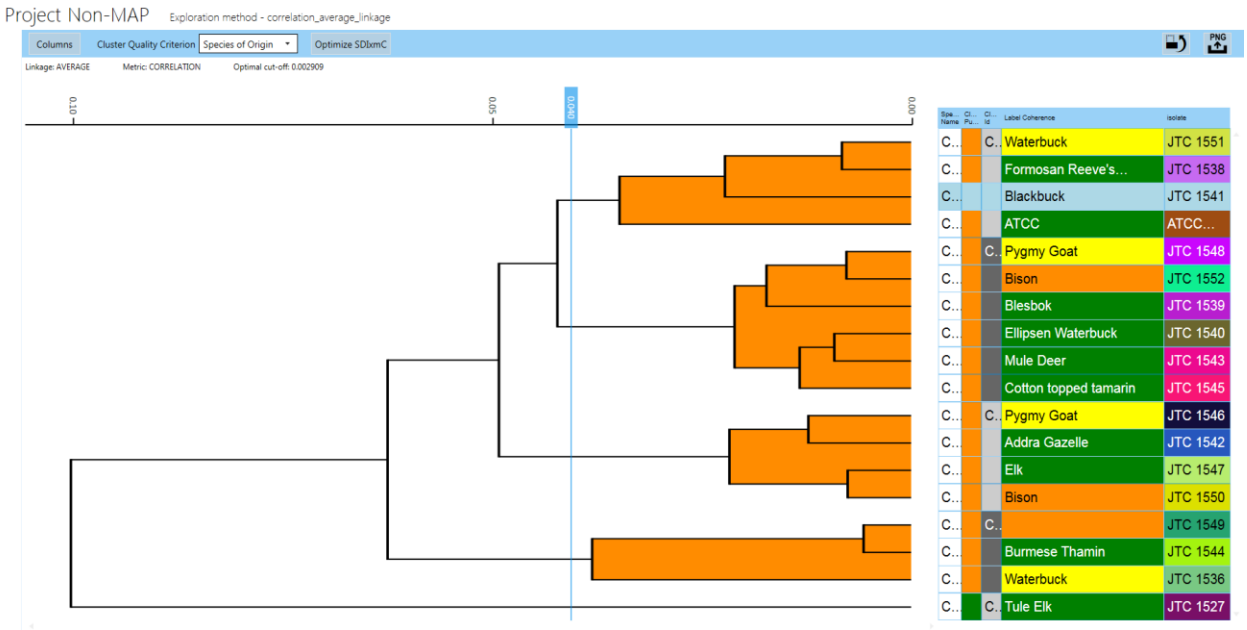

Figure 6: Dendrogram based on the host species of origin of non-MAP. Second column indicates cluster purity signified as green as "good", Orange as "medium", and yellow as "bad". On the top left, the optimal cut off is 0.002, the lowest among three other HCA analysis of this research.

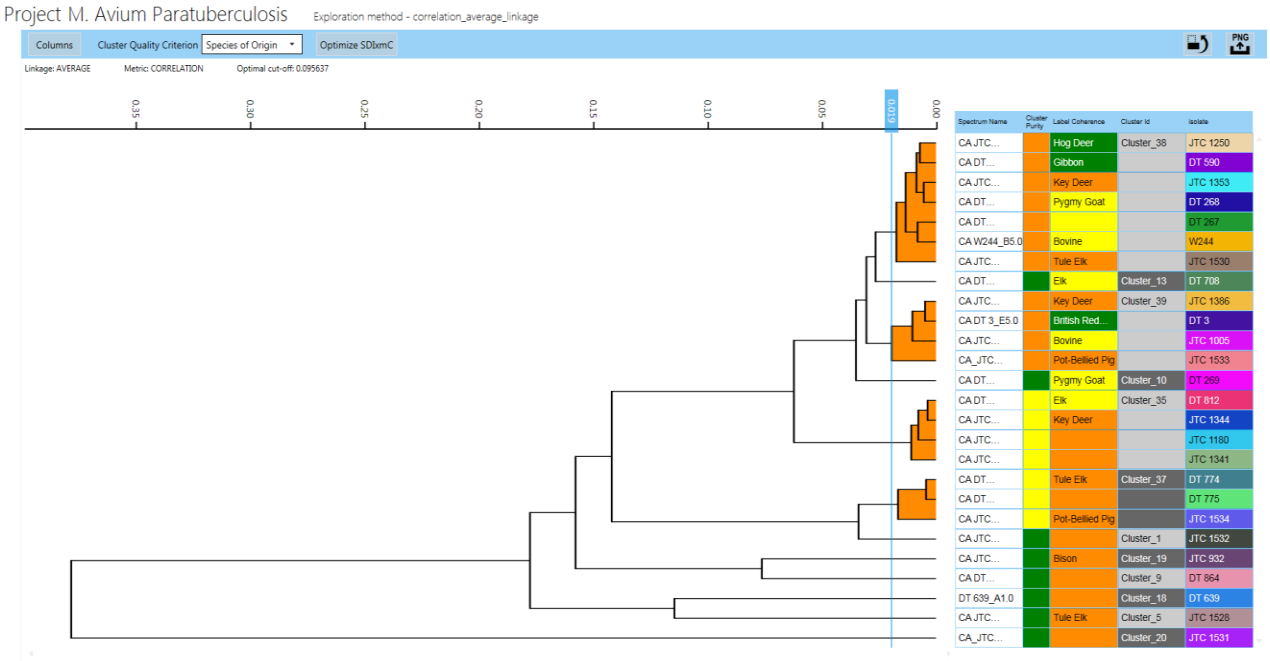

Figure 7: Displaying Hierarchical cluster analysis (HCA) of MAP in relation to the host species of origins. The cluster purity is varied and the optimal cut off is 0.09.

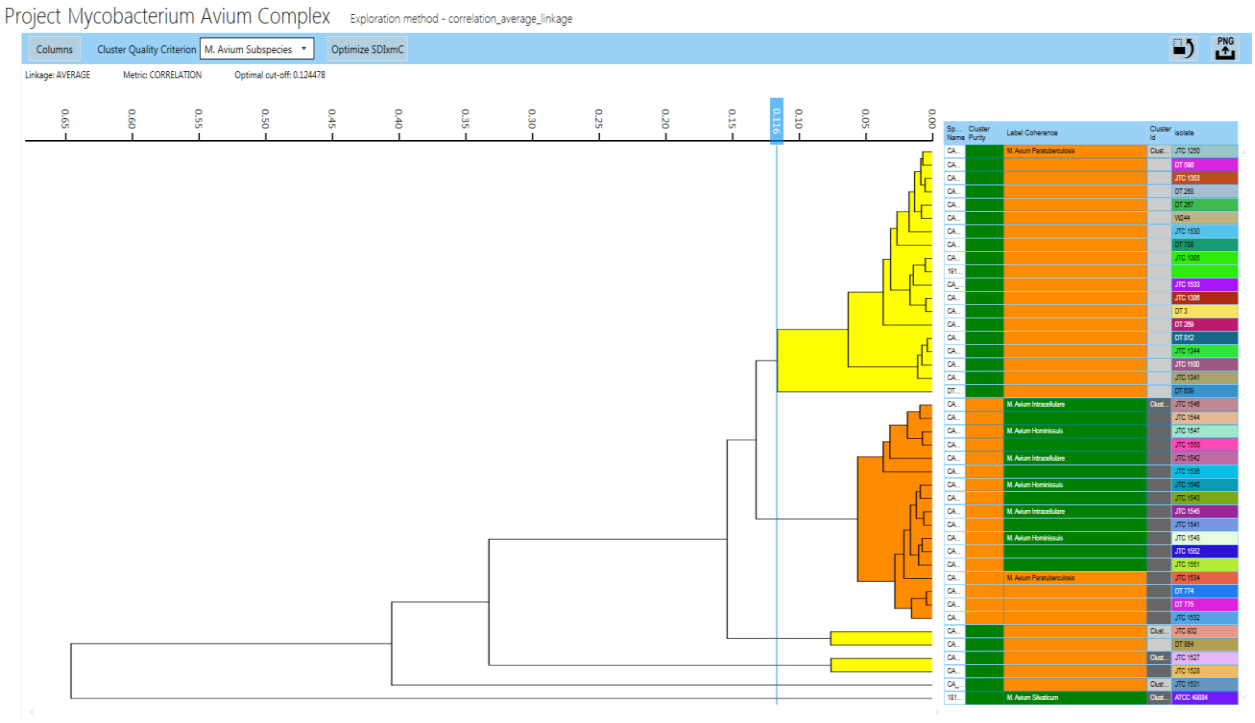

Figure 8: Showing characterization between MAP and non-MAP. The cluster purity of MAP are all green demonstrating “good” purity, except four strains in the middle cluster having orange color (medium). All strains of non-map has orange color representing “medium” purity.

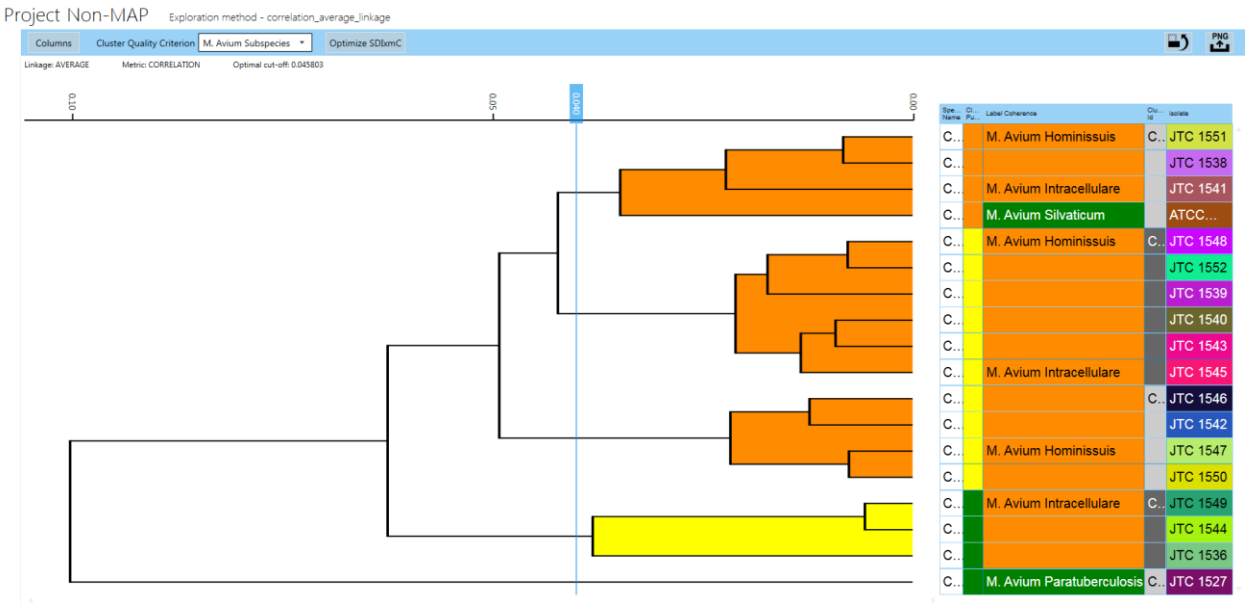

Figure 9: Depicting differentiation of the members of MAC.

B. Chapter 2

4 Background and Literature Review

4.1 General Introduction of Porcine Reproducive and Respiratory Syndrome (PRRS)

Porcine Reproductive and Respiratory Syndrome (PRRS) is one of the most devastating diseases in swine after the eradication of classical swine fever. The history of PRRS began in the late 1980s, where it first emerged in North America. Another lineage appeared in Europe in 1990, continuing to spread globally (Lunney et al., 2010). The etiologic agent of PRRS is PRRS virus—a single-stranded, positive-sense RNA virus belonging to the family *Arteriviridae.* Clinical signs of PRRS include reproductive failure, infertility, birth defects in piglets, severe respiratory disease manifesting in pneumonia, and impaired growth, ultimately sometimes ending in death. PRRSV invades the immune system specifically macrophage in the lung. In some cases, it can promote more severe secondary infections, such as bacterial pneumonia. It has been identified that PRRSV diverged into two types: European lineage (Type 1) and North American lineage (Type 2) (Kappes & Faaberg, 2015). Type 2 appears to have more heterogeneity as compared to Type 1, making it more virulent. Both lineages have only 65 % genetic similarity (Kimpston-Burkgren et al., 2017). Thus, it creates variation between strains. PRRSV variability causes difficulty in control and prevention strategies. Vaccination is one of the most widely used control strategies for PRRSV, but it does not give 100% protection for the herds. Current vaccines, such as modified live vaccine (MLV), could be a successful approach, yet they only works against the strains similar to the corresponding vaccine (Kimpston-Burkgren et al., 2017). As a result, PRRSV is very economically significant since it causes a high level of morbidity, leading to a billion-dollar loss in the swine industry. At present, the transmission of

PRRSV has extended throughout the world, excluding Australia, New Zealand, Brazil, and Switzerland (OIE). In the United States only, the annual losses due to PRRSV infection has been estimated to be $664 million in 2005 to 2010. Further research still needs to be done to understand the more profound characteristic of pathogens in order to develop better solutions in minimizing the spread of the pathogen (World Organization for Animal Health, 2008).

4.1.1 Viral Genome and Structure

The full-length genome of PRRSV has been known to have a total size of 15 kb (Kappes & Faaberg, 2015). The PRRSV genome is a positive sense, single-stranded RNA, which is flanked by a 5' methyl cap and 3' polyadenylated tail (Sun., 2017). There are 11 open reading frames (ORFs) present in the genome. ORF 1a and 1b encode for non-structural proteins, and ORF 2-7 encode for structural proteins. Synthesis of ORF 1a and 1b produces large polyproteins, namely pp1a and pp1ab. The polyprotein pp1a is post-translationally modified into ten functional non-structural proteins (nsps) via cleaving during complex proteolytic cascades. Four putative proteinase domains encoded in ORF 1a instruct this process. The ten functional proteins are nsp1α, nsp1β, nsp2, nsp3, nsp4, nsp5, nsp6, nsp7α, nsp7β, and nsp8. The polyprotein pp1ab undergoes similar proteolytic cascades generating four nsps: nsp9, nsp10, nsp11, and nsp12. A new ORF was recently discovered, namely -1/-2 ribosomal shift signal and Trans Frame (TF), located in the central region of ORF 1a. TF synthesizes two viral proteins: nsp2TF and nsp2N (Li et al., 2014).

The rest of the ORFs are responsible for the PRRSV structure assembly. ORF 2a-4 encode for minor N- glycosylated envelope proteins: GP 2, 3, and 4. The glycoproteins form a heterotrimer linked by disulfide bonds. ORF 5-7 encode for one glycosylated and two non-glycosylated major structural proteins: GP 5, N, and M proteins. GP 5 and M protein interact and

form heterodimers. The minor GPs have been found to bind to cellular receptor CD 163 necessary for viral infectivity (Das et al., 2009). ORF 2b, integrated within ORF 2a, generates E non-glycosylated envelope protein required for viral uncoating and viral release in the cytoplasm. The N (nucleocapsid) protein is a dimer essential for viral particle formation through interaction with the viral genome (Dokland, 2010).

The viral structure of PRRSV is known to be spherical or oval with a diameter of 50-60 nm. Through the cryo-electron microscopy (EM) image, the enveloped surface lacks spike, and the viral glycoproteins embedded in the lipid bilayer surface are exposed. Inside the virus, the genome is enclosed by a capsid. Previous studies indicated PRRSV had icosahedral symmetry, yet Dokland et al. (Dokland, 2010) found that the virus has a loosely filamentous structure of helical coils. Inside the virion, there is a nucleocapsid (N) protein that is forming a two-layered structure with protein dimers linked into a twisted chain with the RNA in the middle (Doan & Dokland, 2003). The RNA genome connects with the N-terminal domain of the nucleocapsid, while the C-domain becomes the foundation of the capsid structure. The N protein is phosphorylated, and it is proposed that it might function for protein interaction and RNA binding(Doan & Dokland, 2003).

4.1.2 Viral Infectivity and Replication

PRRSV has restricted tropism in host cells as it is only able to replicate in a few cell types (Gao et al., 2013). PRRSV is only infectious to porcine alveolar macrophages (PAMs) and developing monocytes. Since primary PRRSV research is usually done using monkey kidney derived cells such as MARC 145 and MA 104, its biological relevance concerning its tropism is still questionable. None of the cell lines used for PRRSV research are derived from porcine, which is one of the PRRSV research discrepancies (Mulupuri et al., 2008).

Several potential PRRSV viral receptors have been discovered, namely sialoadhesin (CD 169), vimentin, heparan sulfate, CD 151, and CD 163 (Kimpston-Burkgren et al., 2017). However, further research might need to be done for four of these receptors, except sialoadhesin and CD 163, which have been extensively studied in the past. The mechanism of viral entry starts with the binding of GP 5/M structural protein to sialoadhesin and heparan sulfate. Then, the interaction of GP 2a protein with CD 163 provides viral attachment and invagination of host cells (Tian et al., 2009). Upon entering the host cell, PRRSV E protein act as an ion channel that senses changing pH. Once pH is under the right condition, it releases signal to uncoat viral particles, exposing the genome (standard clathrin-mediated). In spite of that, it was discovered that CD 169 binding is not necessary for viral entry, but instead, CD 163 is the critical factor of the viral entry (Verheije et al., 2003). Overexpression of CD 163 in several non-permissive cells allows them to become susceptible to infection, which demonstrates that CD 163 is the center of viral entry and attachment.

Viral replication begins in the cytosol after clathrin-mediated endocytosis. Viral membrane fuses into the endosomal layer, then the genome is released. ORF 1a and 1b are translated to form long polyprotein, which subsequently processed to be NSPs (non-structural proteins). NSPs form what are called replication and transcription complexes (RTCs), which accumulate at the virus-induced-ER-derived double-membrane vesicles (Yu et al., 2015). The RTCs then initiate synthesis to produce both full-length and sub-genomic length minus-strand RNA (-sg RNA). The full-length minus-strand RNA will be the template for genome replication. The -sgRNA will function as the template for the synthesis of several sets of sg mRNAs, which are required to generate viral structural proteins. Host ribosomes translate these mRNA for structural proteins. While approaching the late stage of viral replication, N proteins will attach to

newly synthesized viral RNA forming the nucleocapsid complex. After encapsidation, the virion will bud into the Golgi complex and/or lumen of smooth ER. As viral particles accumulate inside the cell, it will be released into extracellular space via exocytosis.

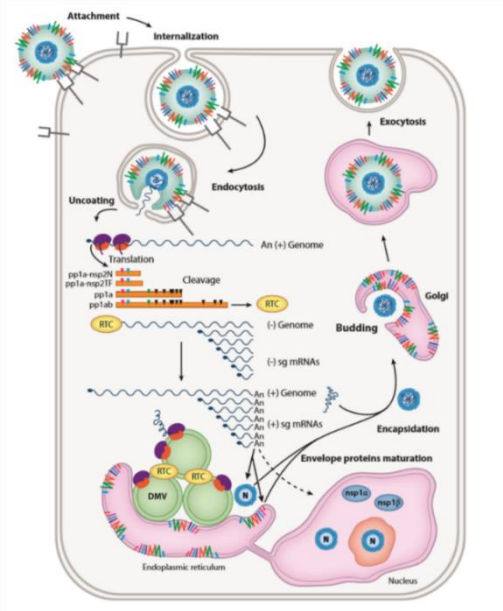

Viral entry and replication of PRRSV. Image courtesy of *Lunney et al.*

4.1.3 Viral Infection and Host Immune Modulation

The early post infection of PRRSV after initial exposure (PI) is described commonly by the presence of several clinical signs and abundant viral loads in the target cells: alveolar and tissue macrophages. This acute phase usually last for up to one month, followed by a late persistent phase. During the late phase, PRRSV replicates to low viral load and it resides primarily in the lymphoid tissues. Ultimately, the virus will be cleared from the body after approximately 150 days after PI or more. The actual mechanism of PRRSV persistence is unknown, but a major influencing factor which causes persistence could be the inability of the host immune response to provide protective immune response (Lopez & Osorio, 2004).

Like other types of viruses, the host immune response will start from innate immune factors such as physical barriers, skin barrier, protease, lipid, and pH. Non-specific white blood cells including natural killer (NK) cells, eosinophils, and macrophages also protect the host and induce an adaptive immune response. The most critical white blood cell at this stage is the NK cell, as it involved in cytotoxicity activity and recruiting T- and B-cells. Sentinel immune cells, such as macrophages and dendritic cells, activate NK cells through the secretion of type 1 Interferon (IFN), Interleukin -12 (IL-12), and cytokines. Activated NK cells will secrete perforin and granzyme to kill target cells that are lacking major histocompatibility class I (MHC-1), and also produce cytokines, like IFN-γ, to recruit adaptive immune cells. PRRSV suppresses production of type 1 IFN in infected pigs. Five PRRSV nonstructural proteins (nsp1α, nsp1β, nsp2, nsp4, and nsp11) and one structural protein (N) are responsible for this inhibition (Nan et al., 2017).

The next line of defense that the host cell would use after an innate immune response is the adaptive immune response. Antigen-presenting cells, such as dendritic cells, will present antigens with MHC class 1 to recruit T-cells and activate B-cells to produce antibodies. Past studies have investigated neutralizing antibodies against homologous PRRSV. Nine-Eleven-days post-infection, it was observed that non-specific immunoglobulin M (IgM) was produced (Gao et al., 2013). Specific antibody, such as IgG response, was detected ten days post-infection. These antibody responses can be more potent for homologous PRRSV. However, for heterologous PRRSV, this immunity is insufficient and won't give reliable protection against both type 1 and type 2 strains.

Immunology research continues to investigate memory B-cells and plasma cells regarding PRRSV infection. Memory B-cells were extracted from tonsil, lymph nodes, and spleen. It was shown that memory B-cells have a robust immune response against nsp2, GP5, and nsp7 viral proteins (Sun., 2017). However, there are still many questions that have not been

answered regarding the immune response of PRRSV. Also, it is not known how the immune response works specifically for the two different types of PRRSV.

It was demonstrated that a significant immune response was caused by structural glycoproteins. Still, recent research using chimeric virus does not give evidence that a potent immune response is only due to glycoprotein (Tian et al., 2009). The researchers suggest that other proteins yet to be discovered may be responsible for inducing a robust immune response.

4.2 Vaccine and Antiviral Strategies

4.2.1 Live Attenuated Viral Vaccines

Knowing the importance of vaccines to reduce the transmission of PRRSV, many studies on vaccines have been conducted. One of the most popular vaccines researched is a live attenuated vaccine. This type of vaccine strategy is known to be the most effective for many different kinds of viruses. One of the main techniques to develop a live-attenuated viral vaccine is to serially passage the virus in another type of cell line to reduce viral infectivity. Upon a certain level of attenuation, the virus can be inoculated into a pig (Verheije et al., 2003). This vaccine is very efficient because it generates a potent immune response even without knowing the specific mechanism of the viral immune modulation or host immunity. However, the disadvantage is that this vaccine can protect only homologous PRRSV. It fails to prevail against heterologous PRRSV. Another attempt to improve vaccine efficacy was done by Verheije and his team. They slightly modified the parental strains of PRRSV by inserting two amino acid residues in the GP2 (Verheije et al., 2003). In addition, they also changed the M protein with murine lactate dehydrogenase found in arterivirus and deleted 6 amino acids of the c terminus of N proteins. These three modified live attenuated viruses were subjected to a challenge study. Nevertheless, these vaccines were found to be ineffective because they could not protect the pigs

against infection after immunization, although they could suppress viremia. Only the second live attenuated vaccine was found to be effective.

Nowadays, the most widely used vaccine is PRRS MLV by Ingelvac. It has been used for several years to suppress the transmission of the virus on farms. Yet, this vaccine does not give broad protection, and it is only valid for the viral strains related to the vaccine. Herd prevalence level is still high, and control is limited (Vu et al., 2015). Surprisingly, the PRRSV live attenuated vaccines fail to give full protection for different types of PRRSV, whereas vaccines from other members of the same arterivirus family, such as equine arteritis virus (EAV), are highly efficient against variation of EAV(Nan et al., 2017).

4.2.2 Synthetic Virus Vaccine Candidate

Another approach that has been taken to extend broader protection against PRRSV is by using chimeric viruses possessing a centralized gene. In a previous study (Vu et al., 2015), a centralized gene was constructed by creating a consensus viral genome from 59 non-redundant, whole-genome sequences of PRRSV type 2. This study was able to create a synthetic virus designated as PRRSV-CON successfully. Results suggest that PRRSV-CON has improved heterologous protection among variants of PRRSV, particularly type 2 PRRSV. Thus, it has potential to be one of the most efficient vaccine candidates. The mechanism of how PRRSV-CON can generate a potent immune response is poorly understood, but it is assumed that the glycoprotein is the main reason. The glycoprotein was described to be a potential molecule inducing an immune response, other proteins may also be involved, such as GP5, M, and N protein. Upon finding the immunity mechanism of PRRSV-CON, similar strategies of vaccination could be employed, except, instead of using a consensus genome, these should focus more on the viral genes that can induce protective immunity.

4.2.3 Antiviral for PRRSV

The current trend of PRRSV research lies in the development of an antiviral. Some effective antivirals have been discovered. Two molecules that are known to inhibit viral replication are miRNA and nanobodies. Zhang and associates found that the miRNA -23 host factor can upregulate type 1 IFN by activating interferon regulatory factor 3 (IRF 3) and IRF 7. The result indicated that miRNA -23 is a potent suppressor of PRRSV infection by directly binding to the PRRSV genome and subgenome in its replication cycle, hence this miRNA could be potential antiviral (Qiong Zhang et al., 2014). Furthermore, miRNA -181 also exhibited inhibition during viral replication by binding to the ORF 4 (Dhorne-Pollet et al., 2019). Despite having antiviral properties, there some particular miRNA that are proviral. For instance, miRNA -373 targets nuclear factor one and other associated kinases. As a result, it will impair IFN β production, which then promotes viral replication into the host. Lastly, recent research found that nanobodies, a single-chain antibody fragment derived from Camelidae heavy chain (VHH), can target specific viral proteins. In the case of PRRSV, the nanobodies bind to nsp9 and nsp4, which are essential for the viral genome. Wang and associates attempted to express this nanobody into MARC 145 cell lines, which, in turn, exhibited antiviral properties against viral proteins, including pp1a and pp1b (Wang et al., 2019). Thus, this antiviral could be a potential treatment for PRRSV infection.

4.3 PRRSV Project Objective

PRRS is one of the major viral diseases responsible for huge economic losses and morbidity in the swine industry. Clinical signs of PRRS include chronic respiratory disease among young pigs as well as a reproductive failure of pregnant sows. The etiologic agent of PRRS is the PRRS virus— a positive single-stranded RNA-enveloped virus. There are two types

of PRRSV circulating worldwide classified as PRRSV-1 (European) and PRRSV-2 (North American). PRRSV has a genome size of approximately 15 kb, with ten open reading frames (ORFs). Genetic variations among PRRSV is common as the virus is prone to mutation. Nevertheless, PRRSV-2 displays greater antigenic heterogeneity than PRRSV-1 exhibiting distinct properties of their surface glycoprotein. Their sequence similarity is 60% (Vu et al., 2015). Multiple variants of PRRSV can easily spread among a herd, imposing considerable challenges for finding optimal vaccine protection. Although various vaccines for PRRSV are already available in the market, none of those vaccines can administer broad protections for both strains. The most effective vaccine—a modified live virus vaccine (MLV) —is made from type 1 PRRSV and will only protect against type 1 PRRSV. It is ineffective against type 2 strains (Kimpston-Burkgren et al., 2017).

To overcome this genetic variation, a well-known vaccine strategy has been developed by generating a synthetic virus vaccine that contains centralized sequences. In a previous study (Vu et al., 2015), consensus viral-genome was constructed from 59 non-redundant, whole-genome sequences of type 2 PRRSV to produce synthetic virus (PRRSV-CON). The study confirmed that PRRSV-CON had broadened the level of protection for type 2 PRRSV strains. However, despite this success, the mechanism of how PRRSV provides immune protection has not been determined. Specifically, it is not clear which viral proteins are capable of eliciting optimum immune responses.

The objective of this project was to study the relative contribution of PRRSV structural proteins in inducing swine immunity through a reverse genetic system. Structural proteins of PRRSV are most likely the contributor of viral infectivity because these proteins are the binding sites of an antibody. Thus, we hypothesize that structural proteins of PRRSV can elicit maximum

immunity. The location of these structural proteins is found in the open reading frame ORF 2 to 7. ORF 2-5 contains surface glycoproteins, and ORF 6-7 bears proteins required for viral particle and capsid formation (Dokland, 2010; Music & Gagnon, 2010).

4.4 Material and Methods

Cells, Antibodies, and PRRSV Strains

MARC-145 cell lines derived from monkey kidney cells were utilized in this experiment. The cells were cultured in Dulbecco's modified Eagle's medium (DMEM) and supplemented with 10% fetal bovine serum (FBS) in the 37 °C incubator with 5% CO2. Type 1, type 2 PRRSV cDNA clones (pSD01-08 and pFL12), DH5α bacterial competent cells, and the monoclonal antibody SDOW 17 for *in vitro* tests were obtained from the stocks of previous research (Kimpston-Burkgren et al., 2017). The secondary antibody—Alexafluor-488 conjugated donkey anti-mouse antibody was purchased from Invitrogen. Plasmid (pUC57-AMP) containing PasI, SbfI, PacI, 3'UTR, HDVRz (hepatitis delta ribozyme), and XbaI sequences were synthesized artificially through a contract with a biotech company for insertion of new restriction sites *(Table 1).*

Method 1: Generation of type 1 modified PRRSV

Due to the absence of the closest restriction sites in ORF 2, a single restriction site (SbfI) was added, as seen in step 1, *Figure 6*. To insert the new restriction site, the pSD01-08 plasmid was digested with PasI and XbaI restriction enzymes, generating three fragments: fragment one from XbaI to PasI#1 site (13,794 bp), fragment two from PasI#1 to PasI#2 site (3,978 bp), and fragment three from PasI#2 to XbaI site (903 bp). Fragment 1 and pUC57-AMP were digested with PasI and XbaI, and the corresponding fragments were ligated. The resulting plasmid had a large deletion from PasI to end of ORF7, designated as an intermediate 1 plasmid. The plasmid

was transformed into DH5α competent cells according to the protocols from New England Biolabs. Positive clones were assessed by digestion and sequencing. Next, the non-structural PRRSV-1 genome was amplified through PCR, including flanking of SbfI site to the reverse primer. The resulting PCR fragment was cloned into the intermediate 1 plasmid to produce intermediate 2 plasmid, which contained SbfI new sites and non-structural protein of PRRSV-1. Furthermore, to complete the genome of PRRSV-1, a second PCR containing the entire structural genes (ORF2-7) of PRRSV-1 was amplified and cloned into the intermediate 2 plasmids, under SbfI and PacI restriction enzyme sites. Positive clones were assessed by digestion and sequencing, as the previous steps. The resulting plasmid containing the full-length sequence of pSD01-08, with the new restriction enzyme inserted at the 5' end of ORF2 and 3' end of ORF7, was designated pmSD01-08.

Method 2: Transfection to recover modified type-1 PRRSV

To recover the virus, pmSD01-08 was transfected into MARC-145 cells, using the TransIT-cDNA transfection kit (Mirus Bio). Prior to transfection, the cells were seeded for 24 h in 6 well plates and observed for confluency. The plasmid was mixed with Opti-MEM reduced serum media and TransIT reagent according to the protocols. The transfected cells were cultured in DMEM containing 10% FBS and incubated at 37 °C with 5% CO2. After 4 hours of incubation, the media on the transfected cells was changed with fresh complete DMEM media, ensuring optimum transfection process. The cytopathic effects (CPE) were evaluated for five days post-transfection, and the supernatant was collected as a stock virus for future studies.

Method 3: Indirect-Immunofluorescence Assay (IFA)

Immunofluorescence assay was performed to evaluate the reactivity of the virus towards PRRSV specific monoclonal antibody (mAB). The transfected cells from the preceding steps

were washed twice with phosphate buffer saline (PBS) (pH 7.4). The cells were fixed with 4°C Acetone-Methanol (1:1) and incubated for 15 minutes, followed drying at room temperature. Next, SDOW17 PRRSV mAB from mouse was added as a primary antibody to the fixed cells and incubated at room temperature in the shaker for one hour. Finally, the secondary antibody (Alexafluor-488 fluorescence conjugated antibody) was administered after washing three times with PBS to remove the primary antibody. The cells were incubated (RT) in the shaker for one hour in addition to wrapping the plates with aluminum foil to prevent the absorption of light. Finally, the fluorescence signal was observed under a fluorescence microscope.

Method 4: Genome swapping of modified type 1 PRRSV and type 2 PRRSV

pFL12 structural genes (ORF 2-7) were amplified by PCR using a pair of primers that contain restriction enzyme SbfI and PacI. The PCR product was cloned into the pmSD01-08 under SbfI and PacI. The resulting synthetic plasmid designated as pSDFL27 had non-structural proteins from PRRSV-1 and structural proteins from PRRSV-2. The subsequent steps were the same as *method 2 and 3*.

4.5 Results

Insertion of Sbf1 restriction sites

There was no closest restriction enzyme found in the pSD01-08 (PRRSV-1), which was the backbone for our construct. Therefore, a short synthetic DNA fragment containing three restriction sites was generated to aid the subsequent cloning steps. The synthetic DNA fragment was synthesized by a biotech company and was delivered in a plasmid labeled pUC57-AMP. This synthetic DNA was successfully added in pSD01-08, displayed in *Figure 1*. *Figure 2* depicts the full-length construct of pmSD0-08 (PRRSV-1) with additional SbfI and PacI sites. There were two positive clones (clones# 2 and #3) for pmSD01-08. These two clones were

digested with several restriction enzymes to confirm their authenticity *(Figure 4)*. Lane 1, the clones were cut with SbfI and AscI; lane 2 with AscI and EcoRV; lane 3 with SbfI and EcoRV. The size of the bands was similar to the gel simulation in software SnapGene. Moreover, two plasmids (intermediate1 and pmSD01-08) were run into the gel electrophoresis to verify the integration of non-structural proteins and structural protein sequences (ORF 2-7) of PRRSV-1 into intermediate 1 *(Figure 3)*. The intermediate 1 has lower base pairs than pmSD01-08. Hence, in lane 1 *(Figure 3)*, the band moves further.

Modified type-1 PRRSV (pmSD01-08) Recovery

Validation whether pmSD01-08 is infectious was done by transfecting the plasmid into MARC-145 cells. After five days of transfection, CPE was spotted in the light microscope, suggesting pmSD01-08 to be infectious. Therefore, we conducted immunofluorescence assay (IFA) with an antibody specific for PRRSV from the infected mouse to prove the infectivity of the cells. To control the transfection efficiency, a plasmid encoding green-fluorescence protein (GFP) was included. *Figure 5A* exhibits the fluorescence signal observed from the well transfected with GFP plasmid. For positive control, an infectious clone designated NCV1 that is known to produce infectious virus after transfection was used. The strong fluorescence signal was observed from cells transfected with the NCV1 infectious clone *(Fig. 5B)*. Finally, *Fig 5C* and *5D* show the fluorescence signal observed from cells transfected with the pmSD01-08 plasmid clone#2 *(Fig 5C)* and clone#3 *(Fig 5D)*. Both clone# 2 and clone#3 were infectious since it is bound to the antibody and emitted green fluorescence. Clone#3 *(Fig 5D)* appears to be more infectious than clone#2 *(Fig 5C)* based on the observation in immunofluorescent microscope.

Recombinant PRRSV (pSDFL27) is not infectious.

Confirmation of *pm SD01-08* from the previous step enabled the production of chimeric plasmid called pSDFL27. This plasmid contained the genome of non-structural proteins from PRRSV-1 and structural protein from PRRSV-2. PRRSV-1 functions as a vector to express PRRSV-2 structural proteins in this case. After transfection in MARC-145 as in *method 3*, the result from pSDFL27 transfected cells showed no CPE. IFA also verified this result, as shown in *Figure 7*. No green fluorescence light emanated (Fig 7A). Thus, the virus was not produced in the cell and no antibody binding to the virus. This construct pSDFL27 was not infectious and could not be recovered in the cells.

4.6 Discussion

The mechanism by which PRRSV induces immune protection remains unclear in vaccinated or wildly infected swine. Previous research has assessed the four highly variable GP of PRRSV located in ORF 2-4 (Kimpston-Burkgren et al., 2017). Nevertheless, the antibody raised against these glycoproteins is not fully neutralizing, implying that other proteins play a role in the antibody neutralization. Thus, in this research, we hypothesized that the whole structural proteins of PRRSV (ORF 2-7) are involved in the induction of antibodies. The proteins produced from ORF 5-7 may have potential epitopes that can bind to the antibody. ORF 5 produces GP 5, and ORF 6 encodes for M proteins, and ORF 7 generates N protein dimers. GP 5 and M protein form heterodimers that have been known to interact with sialoadhesin (van Breedam et al., 2010). The N-protein cooperates with the viral genome to viral assembly particles. All of these proteins have been reported to have significant roles in viral infectivity (Qingzhan Zhang & Yoo, 2015). In this study, we used PRRSV-1 strain (pSD01-08) as the backbone of the viral vector to deliver the whole structural protein of PRRSV-2 strain. As both

strains have less genetic similarity, they are not cross-protecting (Choi et al., 2016). Therefore, the pSD01-08 infectious clone (PRRSV-1) is suitable for the expression of the PRRSV-2 structural genes because it will produce the structural proteins in their biological forms. The construct for the vector required insertion of restriction sites to enable swapping between both strains. We successfully modified the vector pmSD01-08 with these new insertion sites *(Figure 1)*, and the vector could be demonstrated in the MARC-145 cell *(Figure 5)*. The construction of pSDFL-27 was done after swapping structural proteins of the vector with PRRSV-2. However, in the transfection step, pSDFL 27 was not infectious, as in *Figure 7*. This occurred possibly due to the substitution of N-protein (ORF 7) between type 1 and typed 2 PRRSV in pSDFL27 interfering viral assembly.

N-protein is a viral nucleocapsid required for viral particle formation. This protein assists the structural proteins to interact and assemble with the viral genome, producing a complete infectious viral particle (Music & Gagnon, 2010). A study demonstrated that viral RNA synthesis is regulated by the interaction of N-protein and Nsp9 (Liu et al., 2016). Therefore, pSDFL27 failed to be recovered in the cells, possibly because the assembly of the viral particle was hindered. The replacement ORF-7 of PRRSV-1 with ORF-7 of PRRSV-2 will result in the production of N-protein of PRRSV-2 and Nsp9 from the backbone of PRRSV-1. These two proteins from distinct strains may possess different characteristics, which can impede the signaling process and RNA synthesis during the assembly. Hence, there was no viral particle produced in the cells. Furthermore, another study clarifies ORF-7 of PRRSV-2 is conserved (Meng et al., 1995). This indicates that the nucleocapsid of PRRSV-2 can only assemble with the viral genome of PRRSV-2, and vice versa (Meng et al., 1995).

4.7 Conclusion

In conclusion, chimeric pSDFL27 was not able to replicate when transfected into cells, demonstrating that some proteins within ORF 2-7 play significant roles in viral replication and assembly. Thus, these cannot be put in a vector from a different strain. N-protein could be one crucial protein that is not reciprocal between types. Assessment of immune-response induction is still unclear at this point since the chimeric virus failed to recover. However, these results could further the knowledge regarding the reverse genetic system designed in this experiment, and they suggest that the viral vector from the same virus species, but a composite of different strains, also has limitations in terms of its capability to deliver proteins from viruses with significant genetic differences.

4.8 List of Figures and Tables

Restriction Sites	**Sequences**
PasI (cut in two sites)	Cccaggg
PacI	Ttaattaa
SbfI (new site)	Cctgcagg
XbaI	Tctaga

Table 1: displayed significant restriction site with the sequences for plasmid constructs in this experiment. SbfI (red) is the new insertion site.

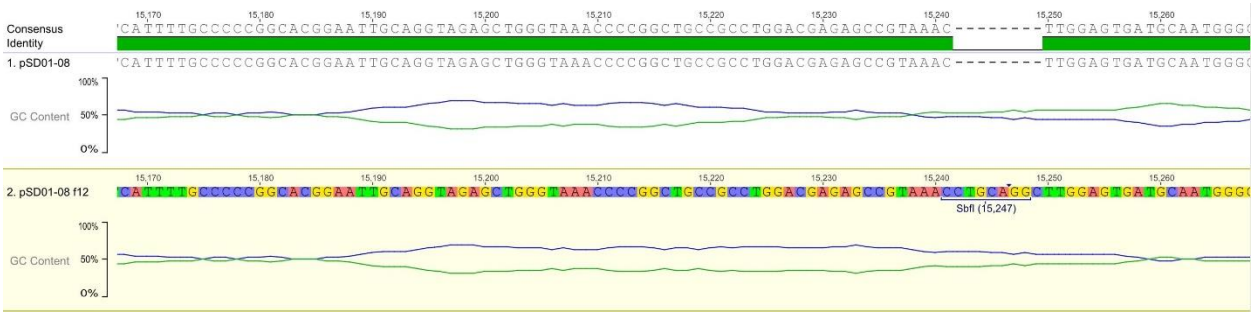

Figure 1: pSD01-08 (PRRSV-1) backbone does not have restriction site SbfI. Pm SD01-08 (bottom) was confirmed to have SbfI site.

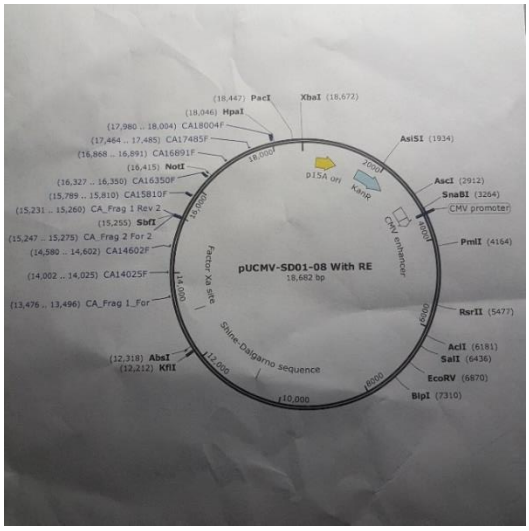

Figure 2: full-length modified plasmid pmSD01-08 with Sbf1 and PacI sites.

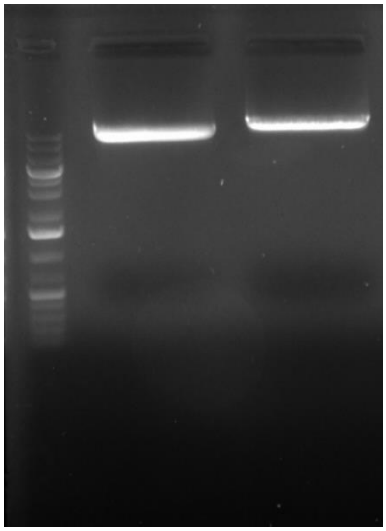

Figure 3: showed the gel electrophoresis results from intermediate 1 and pm SD01-08. The left band is intermediate 1, having less base pairs than the right band (pmSD01-08).

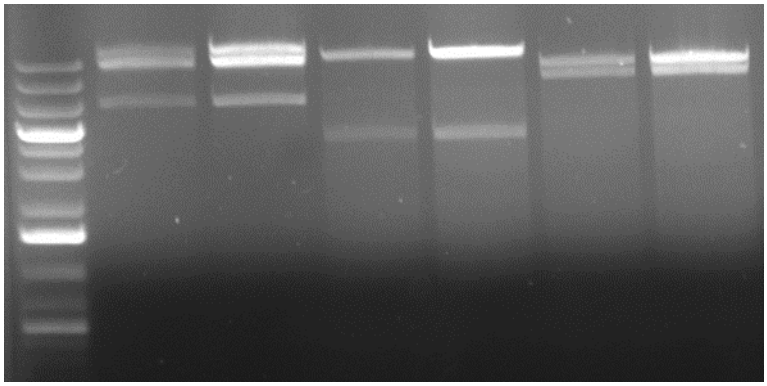

Figure 4: Lane 1,3,5 correspond to clone #2 (pmSD01-08) and lane 2,4,6 correspond to clone #3 (pmSD01-08). Both clones were digested with several restriction enzymes (SbfI, EcoRV, AscI) to ensure the presence of new insertion site and full-genome of PRRSV-1.

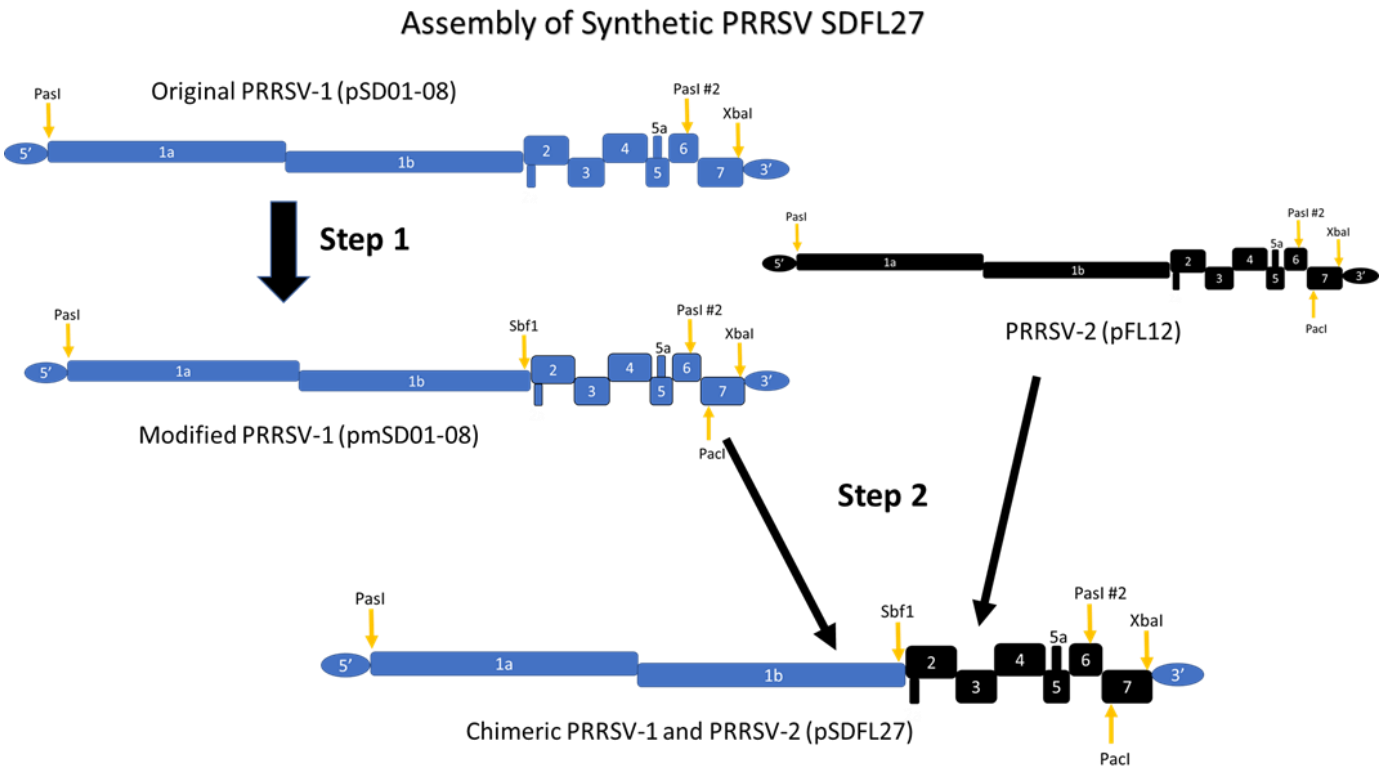

Figure 6: there are two steps involved to create synthetic PRRSV pSDFL27. The first step is insertion of SbfI site and the second step is swapping of ORF 2-7 between pSD01-08(PRRSV-1) and pFL12 (PRRSV-2).

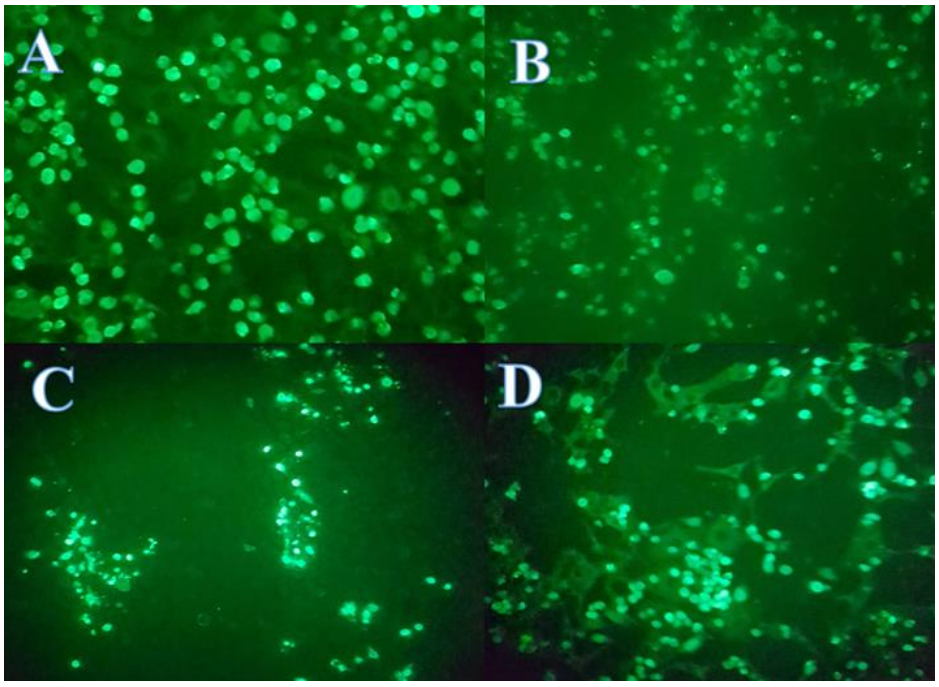

Figure 5: showed GFP expressed cell (A), NCV1 infectious clone (B) as positive control, pm SD01-08 clone#2 (C), and pm SD01-08 clone#3 (D).

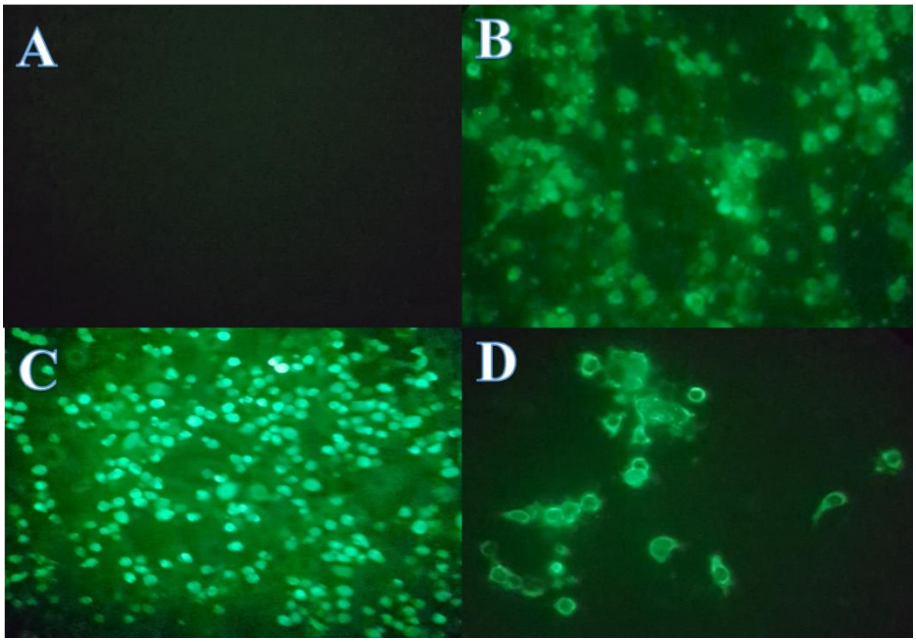

Figure 7: depicted pSDFL27 is not infectious (fig 7A), GFP expressed well in cell (fig 7C), and both positive control of NCV1 and pmSD01-08 produced fluorescence (fig 7D)

5. References

Alatoom, A. A., Cunningham, S. A., Ihde, S. M., Mandrekar, J., & Patel, R. (2011). Comparison of direct colony method versus extraction method for identification of gram-positive cocci by use of Bruker Biotyper matrix-assisted laser desorption ionization-time of flight mass spectrometry. *Journal of Clinical Microbiology*, *49*(8), 2868–2873. https://doi.org/10.1128/JCM.00506-11

Alonso-Hearn, M., Abendaño, N., Ruvira, M. A., Aznar, R., Landin, M., & Juste, R. A. (2017). Mycobacterium avium subsp. paratuberculosis (Map) Fatty Acids Profile Is Strain-Dependent and Changes Upon Host Macrophages Infection. *Frontiers in Cellular and Infection Microbiology*, *7*, 89. https://doi.org/10.3389/fcimb.2017.00089

Arbeit, R. D., Slutsky, A., Barber, T. W., Maslow, J. N., Niemczyk, S., Falkinham, J. O., O'Connor, G. T., & von Reyn, C. F. (1993). Genetic Diversity among Strains of Mycobacterium avium Causing Monoclonal and Polyclonal Bacteremia in Patients with AIDS. *The Journal of Infectious Diseases*, *167*(6), 1384–1390. http://www.jstor.org/stable/30112740

Balasuriya, U. B. R., & MacLachlan, N. J. (2004). The immune response to equine arteritis virus: potential lessons for other arteriviruses. *Veterinary Immunology and Immunopathology*, *102*(3), 107—129. https://doi.org/10.1016/j.vetimm.2004.09.003

Balka, G., Podgórska, K., Brar, M. S., Bálint, Á., Cadar, D., Celer, V., Dénes, L., Dirbakova, Z., Jedryczko, A., Márton, L., Novosel, D., Petrović, T., Sirakov, I., Szalay, D., Toplak, I., Leung, F. C.-C., & Stadejek, T. (2018). Genetic diversity of PRRSV 1 in Central Eastern Europe in 1994-2014: origin and evolution of the virus in the region. *Scientific Reports*, *8*(1), 7811. https://doi.org/10.1038/s41598-018-26036-w

Barfoed, A. M., Blixenkrone-Møller, M., Jensen, M. H., Bøtner, A., & Kamstrup, S. (2004). DNA vaccination of pigs with open reading frame 1–7 of PRRS virus. *Vaccine*, *22*(27), 3628–3641. https://doi.org/https://doi.org/10.1016/j.vaccine.2004.03.028

Bastida, F., & Juste, R. A. (2011). Paratuberculosis control: a review with a focus on vaccination. *Journal of Immune Based Therapies and Vaccines*, *9*, 8. https://doi.org/10.1186/1476-8518-9-8

Bates, A., O'Brien, R., Liggett, S., & Griffin, F. (2019). Control of Mycobacterium avium subsp. paratuberculosis infection on a New Zealand pastoral dairy farm. *BMC Veterinary Research*, *15*(1), 266. https://doi.org/10.1186/s12917-019-2014-6

Biet, F., Boschiroli, M. L., Thorel, M. F., & Guilloteau, L. A. (2005). Zoonotic aspects of Mycobacterium bovis and Mycobacterium avium-intracellulare complex (MAC). *Vet. Res.*, *36*(3), 411–436. https://doi.org/10.1051/vetres:2005001

Bosch, A., Miñán, A., Vescina, C., Degrossi, J., Gatti, B., Montanaro, P., Messina, M., Franco, M., Vay, C., Schmitt, J., Naumann, D., & Yantorno, O. (2008). Fourier transform infrared spectroscopy for rapid identification of nonfermenting gram-negative bacteria isolated from sputum samples from cystic fibrosis patients. *Journal of Clinical Microbiology*, *46*(8), 2535–2546. https://doi.org/10.1128/JCM.02267-07

Bryant, J. M., Thibault, V. C., Smith, D. G. E., McLuckie, J., Heron, I., Sevilla, I. A., Biet, F., Harris, S. R., Maskell, D. J., Bentley, S. D., Parkhill, J., & Stevenson, K. (2016). Phylogenomic exploration of the relationships between strains of Mycobacterium avium subspecies paratuberculosis. *BMC Genomics*, *17*(1), 79. https://doi.org/10.1186/s12864-015-2234-5

Burkard, C., Opriessnig, T., Mileham, A. J., Stadejek, T., Ait-Ali, T., Lillico, S. G., Whitelaw, C. B. A., & Archibald, A. L. (2018). Pigs Lacking the Scavenger Receptor Cysteine-Rich Domain 5 of CD163 Are Resistant to Porcine Reproductive and Respiratory Syndrome Virus 1 Infection. *Journal of Virology*, *92*(16), e00415-18. https://doi.org/10.1128/JVI.00415-18

Carbonnelle, E., Beretti, J.-L., Cottyn, S., Quesne, G., Berche, P., Nassif, X., & Ferroni, A. (2007). Rapid identification of Staphylococci isolated in clinical microbiology laboratories by matrix-assisted laser desorption ionization-time of flight mass spectrometry. *Journal of Clinical Microbiology*, *45*(7), 2156–2161. https://doi.org/10.1128/JCM.02405-06

Chang, C.-C., Yoon, K.-J., Zimmerman, J. J., Harmon, K. M., Dixon, P. M., Dvorak, C. M. T., & Murtaugh, M. P. (2002). Evolution of Porcine Reproductive and Respiratory Syndrome Virus during Sequential Passages in Pigs. *Journal of Virology*, *76*(10), 4750 LP – 4763. https://doi.org/10.1128/JVI.76.10.4750-4763.2002

Charerntantanakul, W. (2006). *Cell-mediated immune response to porcine reproductive and respiratory syndrome virus*.

Chatterjee, D. (1997). The mycobacterial cell wall: structure, biosynthesis and sites of drug action. *Current Opinion in Chemical Biology*, *1*(4), 579–588. https://doi.org/https://doi.org/10.1016/S1367-5931(97)80055-5

Choi, K., Park, C., Jeong, J., & Chae, C. (2016). Comparison of protection provided by type 1 and type 2 porcine reproductive and respiratory syndrome field viruses against homologous and heterologous challenge. *Veterinary Microbiology*, *191*, 72—81. https://doi.org/10.1016/j.vetmic.2016.06.003

Croxatto, A., Prod'hom, G., & Greub, G. (2012). Applications of MALDI-TOF mass spectrometry in clinical diagnostic microbiology. *FEMS Microbiology Reviews*, *36*(2), 380–407. https://doi.org/10.1111/j.1574-6976.2011.00298.x

Croxatto, A., Prod'hom, G., & Greub, G. (2012). Applications of MALDI-TOF mass spectrometry in clinical diagnostic microbiology. *FEMS Microbiology Reviews*, *36*(2), 380–407. https://doi.org/10.1111/j.1574-6976.2011.00298.x

Das, P., Dinh, P., Ansari, I., Lima, M., Osorio, F., & Pattnaik, A. (2009). The Minor Envelope Glycoproteins GP2a and GP4 of Porcine Reproductive and Respiratory Syndrome Virus Interact with the Receptor CD163. *Journal of Virology*, *84*, 1731–1740. https://doi.org/10.1128/JVI.01774-09

Davis, R., & Mauer, L. J. (2010). Fourier Transform Infrared (FT-IR) Spectroscopy: A Rapid Tool for Detection and Analysis of Foodborne Pathogenic Bacteria. In *Current Research, Technology and Education Topics in Applied Microbiology and Microbial Biotechnology Volume 2* (Vol. 2, pp. 1582–1594).

de Alegría Puig, C. R., Pilares, L., Marco, F., Vila, J., Martínez-Martínez, L., & Navas, J. (2017). Comparison of the Vitek MS and Bruker Matrix-Assisted Laser Desorption Ionization-Time of Flight Mass Spectrometry Systems for Identification of Rhodococcus equi and Dietzia spp. *Journal of Clinical Microbiology*, *55*(7), 2255–2260. https://doi.org/10.1128/JCM.00377-17

De Voss, J. J., Rutter, K., Schroeder, B. G., & Barry 3rd, C. E. (1999). Iron acquisition and metabolism by mycobacteria. *Journal of Bacteriology*, *181*(15), 4443–4451. https://pubmed.ncbi.nlm.nih.gov/10419938

Dhorne-Pollet, S., Crisci, E., Mach, N., Renson, P., Jaffrézic, F., Marot, G., Maroilley, T., Moroldo, M., Lecardonnel, J., Blanc, F., Bertho, N., Bourry, O., & Giuffra, E. (2019). The miRNA-targeted transcriptome of porcine alveolar macrophages upon infection with Porcine Reproductive and Respiratory Syndrome Virus. *Scientific Reports*, *9*(1), 3160. https://doi.org/10.1038/s41598-019-39220-3

Dickey, A. M., Schuller, G., Loy, J. D., & Clawson, M. L. (2018). Whole genome sequencing of Moraxella bovoculi reveals high genetic diversity and evidence for interspecies recombination at multiple loci. *PloS One*, *13*(12), e0209113–e0209113. https://doi.org/10.1371/journal.pone.0209113

Doan, D. N. P., & Dokland, T. (2003). Structure of the nucleocapsid protein of porcine reproductive and respiratory syndrome virus. *Structure*, *11*(11), 1445–1451. https://doi.org/10.1016/j.str.2003.09.018

Dokland, T. (2010). The structural biology of PRRSV. *Virus Research*, *154*(1–2), 86–97. https://doi.org/10.1016/j.virusres.2010.07.029

Erume, J., Spergser, J., & Rosengarten, R. (2001). Rapid detection of Mycobacterium avium subsp. paratuberculosis from cattle and zoo animals by nested PCR. *African Health Sciences*, *1*(2), 83–89. https://pubmed.ncbi.nlm.nih.gov/12789121

Evans, A. B., Loyd, H., Dunkelberger, J. R., Van Tol, S., Bolton, M. J., Dorman, K. S., Dekkers, J. C. M., & Carpenter, S. (2017). Antigenic and biological characterization of ORF2-6 variants at early times following PRRSV infection. *Viruses*, *9*(5). https://doi.org/10.3390/v9050113

Fernández-Silva, J. A., Abdulmawjood, A., & Bülte, M. (2011). Diagnosis and Molecular Characterization of Mycobacterium avium subsp. paratuberculosis from Dairy Cows in Colombia. *Veterinary Medicine International*, *2011*, 352561. https://doi.org/10.4061/2011/352561

Gao, L., Guo, X., Wang, L., Zhang, Q., Li, N., Chen, X., Wang, Y., & Feng, W. (2013). MicroRNA 181 Suppresses Porcine Reproductive and Respiratory Syndrome Virus (PRRSV) Infection by Targeting PRRSV Receptor CD163. *Journal of Virology*, *87*(15), 8808 LP – 8812. https://doi.org/10.1128/JVI.00718-13

Garcia, A. B., & Shalloo, L. (2015). Invited review: The economic impact and control of paratuberculosis in cattle. *Journal of Dairy Science*, *98*(8), 5019–5039. https://doi.org/10.3168/jds.2014-9241

Grunert, T., Wenning, M., Barbagelata, M. S., Fricker, M., Sordelli, D. O., Buzzola, F. R., & Ehling-Schulz, M. (2013). Rapid and reliable identification of Staphylococcus aureus capsular serotypes by means of artificial neural network-assisted Fourier transform infrared spectroscopy. *Journal of Clinical Microbiology*, *51*(7), 2261–2266. https://doi.org/10.1128/JCM.00581-13

Hooff, G. P., van Kampen, J. J. A., Meesters, R. J. W., van Belkum, A., Goessens, W. H. F., & Luider, T. M. (2012). Characterization of β-Lactamase Enzyme Activity in Bacterial Lysates using MALDI-Mass Spectrometry. *Journal of Proteome Research*, *11*(1), 79–84. https://doi.org/10.1021/pr200858r

Hussain, T., Shah, S. Z. A., Zhao, D., Sreevatsan, S., & Zhou, X. (2016). The role of IL-10 in Mycobacterium avium subsp. paratuberculosis infection. *Cell Communication and Signaling : CCS*, *14*(1), 29. https://doi.org/10.1186/s12964-016-0152-z

Jungersen, G., Mikkelsen, H., & Grell, S. N. (2012). Use of the johnin PPD interferon-gamma assay in control of bovine paratuberculosis. *Veterinary Immunology and Immunopathology*, *148*(1–2), 48—54. https://doi.org/10.1016/j.vetimm.2011.05.010

Kappes, M. A., & Faaberg, K. S. (2015). PRRSV structure, replication and recombination: Origin of phenotype and genotype diversity. *Virology*, *479–480*, 475–486. https://doi.org/https://doi.org/10.1016/j.virol.2015.02.012

Kimpston-Burkgren, K., Correas, I., Osorio, F. A., Steffen, D., Pattnaik, A. K., Fang, Y., & Vu, H. L. X. (2017). Relative contribution of porcine reproductive and respiratory syndrome virus open reading frames 2–4 to the induction of protective immunity. *Vaccine*, *35*(34), 4408–4413. https://doi.org/https://doi.org/10.1016/j.vaccine.2017.06.061

Krishnan, M. Y., Manning, E. J. B., & Collins, M. T. (2009). Comparison of three methods for susceptibility testing of Mycobacterium avium subsp. paratuberculosis to 11 antimicrobial drugs. *Journal of Antimicrobial Chemotherapy*, *64*(2), 310–316. https://doi.org/10.1093/jac/dkp184

Krzywinska, E., Bhatnagar, S., Sweet, L., Chatterjee, D., & Schorey, J. S. (2005). Mycobacterium avium 104 deleted of the methyltransferase D gene by allelic replacement lacks serotype-specific glycopeptidolipids and shows attenuated virulence in mice. *Molecular Microbiology*, *56*(5), 1262–1273. https://doi.org/10.1111/j.1365-2958.2005.04608.x

Kunze, Z. M., Portaels, F., & McFadden, J. J. (1992). Biologically distinct subtypes of Mycobacterium avium differ in possession of insertion sequence IS901. *Journal of Clinical Microbiology*, *30*(9), 2366–2372. https://pubmed.ncbi.nlm.nih.gov/1328288

Lee-Montiel, F. T., Reynolds, K. A., & Riley, M. R. (2011). Detection and quantification of poliovirus infection using FTIR spectroscopy and cell culture. *Journal of Biological Engineering*, *5*(1), 16. https://doi.org/10.1186/1754-1611-5-16

Li, Y., Treffers, E. E., Napthine, S., Tas, A., Zhu, L., Sun, Z., Bell, S., Mark, B. L., van Veelen, P. A., van Hemert, M. J., Firth, A. E., Brierley, I., Snijder, E. J., & Fang, Y. (2014). Transactivation of programmed ribosomal frameshifting by a viral protein. *Proceedings of the National Academy of Sciences of the United States of America*, *111*(21), E2172–E2181. https://doi.org/10.1073/pnas.1321930111

Li, Y., Danelishvili, L., Wagner, D., Petrofsky, M., & Bermudez, L. E. (2010). Identification of virulence determinants of Mycobacterium avium that impact on the ability to resist host killing mechanisms. *Journal of Medical Microbiology*, *59*(Pt 1), 8–16. https://doi.org/10.1099/jmm.0.012864-0

Liu, H., Du, Z., Wang, J., & Yang, R. (2007). Universal sample preparation method for characterization of bacteria by matrix-assisted laser desorption ionization-time of flight mass spectrometry. *Applied and Environmental Microbiology*, *73*(6), 1899–1907. https://doi.org/10.1128/AEM.02391-06

Liu, L., Tian, J., Nan, H., Tian, M., Li, Y., Xu, X., Huang, B., Zhou, E., Hiscox, J. A., & Chen, H. (2016). Porcine Reproductive and Respiratory Syndrome Virus Nucleocapsid Protein Interacts with Nsp9 and Cellular DHX9 To Regulate Viral RNA Synthesis. *Journal of Virology*, *90*(11), 5384–5398. https://doi.org/10.1128/JVI.03216-15

Lopez, O. J., & Osorio, F. A. (2004). Role of neutralizing antibodies in PRRSV protective immunity. *Veterinary Immunology and Immunopathology*, *102*(3), 155–163. https://doi.org/10.1016/j.vetimm.2004.09.005

Lunney, J. K., Benfield, D. A., & Rowland, R. R. R. (2010). Porcine reproductive and respiratory syndrome virus: An update on an emerging and re-emerging viral disease of swine. *Virus Research*, *154*(1), 1–6. https://doi.org/https://doi.org/10.1016/j.virusres.2010.10.009

Lunney, J. K., Fang, Y., Ladinig, A., Chen, N., Li, Y., Rowland, B., & Renukaradhya, G. J. (2016). Porcine Reproductive and Respiratory Syndrome Virus (PRRSV): Pathogenesis and Interaction with the Immune System. *Annual Review of Animal Biosciences*, *4*(1), 129–154. https://doi.org/10.1146/annurev-animal-022114-111025

Mancini, N., De Carolis, E., Infurnari, L., Vella, A., Clementi, N., Vaccaro, L., Ruggeri, A., Posteraro, B., Burioni, R., Clementi, M., & Sanguinetti, M. (2013). Comparative evaluation of the Bruker Biotyper and Vitek MS matrix-assisted laser desorption ionization-time of flight (MALDI-TOF) mass spectrometry systems for identification of yeasts of medical importance. *Journal of Clinical Microbiology*, *51*(7), 2453–2457. https://doi.org/10.1128/JCM.00841-13

Martelli, P., Gozio, S., Ferrari, L., Rosina, S., De Angelis, E., Quintavalla, C., Bottarelli, E., & Borghetti, P. (2009). Efficacy of a modified live porcine reproductive and respiratory syndrome virus (PRRSV) vaccine in pigs naturally exposed to a heterologous European (Italian cluster) field strain: Clinical protection and cell-mediated immunity. *Vaccine*, *27*(28), 3788–3799. https://doi.org/https://doi.org/10.1016/j.vaccine.2009.03.028

McNees, A. L., Markesich, D., Zayyani, N. R., & Graham, D. Y. (2015). Mycobacterium paratuberculosis as a cause of Crohn's disease. *Expert Review of Gastroenterology & Hepatology*, *9*(12), 1523–1534. https://doi.org/10.1586/17474124.2015.1093931

Meng, X. J., Paul, P. S., Halbur, P. G., & Lum, M. A. (1995). Phylogenetic analyses of the putative M (ORF 6) and N (ORF 7) genes of porcine reproductive and respiratory syndrome virus (PRRSV): implication for the existence of two genotypes of PRRSV in the U.S.A. and Europe. *Archives of Virology*, *140*(4), 745–755. https://doi.org/10.1007/bf01309962

Mijs, W., de Haas, P., Rossau, R., der Laan, T., Rigouts, L., Portaels, F., & van Soolingen, D. (2002). Molecular evidence to support a proposal to reserve the designation Mycobacterium avium subsp. avium for bird-type isolates and 'M. avium subsp. hominissuis' for the human/porcine type of M. avium. *International Journal of Systematic and Evolutionary Microbiology*, *52*(5), 1505–1518. https://doi.org/https://doi.org/10.1099/00207713-52-5-1505

Miller, R. S., Sweeney, S. J., Slootmaker, C., Grear, D. A., Di Salvo, P. A., Kiser, D., & Shwiff, S. A. (2017). Cross-species transmission potential between wild pigs, livestock, poultry, wildlife, and humans: implications for disease risk management in North America. *Scientific Reports*, *7*(1), 7821. https://doi.org/10.1038/s41598-017-07336-z

Mulupuri, P., Zimmerman, J. J., Hermann, J., Johnson, C. R., Cano, J. P., Yu, W., Dee, S. A., & Murtaugh, M. P. (2008). Antigen-specific B-cell responses to porcine reproductive and

respiratory syndrome virus infection. *Journal of Virology*, *82*(1), 358—370. https://doi.org/10.1128/JVI.01023-07

Murray, P. R. (2012). What is new in clinical microbiology-microbial identification by MALDI-TOF mass spectrometry: a paper from the 2011 William Beaumont Hospital Symposium on molecular pathology. *The Journal of Molecular Diagnostics : JMD*, *14*(5), 419–423. https://doi.org/10.1016/j.jmoldx.2012.03.007

Music, N., & Gagnon, C. A. (2010). The role of porcine reproductive and respiratory syndrome (PRRS) virus structural and non-structural proteins in virus pathogenesis. *Animal Health Research Reviews*, *11*(2), 135–163. https://doi.org/DOI: 10.1017/S1466252310000034

Nan, Y., Wu, C., Gu, G., Sun, W., Zhang, Y.-J., & Zhou, E.-M. (2017). Improved Vaccine against PRRSV: Current Progress and Future Perspective. *Frontiers in Microbiology*, *8*, 1635. https://doi.org/10.3389/fmicb.2017.01635

Naser, S. A., Sagramsingh, S. R., Naser, A. S., & Thanigachalam, S. (2014). Mycobacterium avium subspecies paratuberculosis causes Crohn's disease in some inflammatory bowel disease patients. *World Journal of Gastroenterology*, *20*(23), 7403–7415. https://doi.org/10.3748/wjg.v20.i23.7403

Nelsen, C. J., Murtaugh, M. P., & Faaberg, K. S. (1999). Porcine Reproductive and Respiratory Syndrome Virus Comparison: Divergent Evolution on Two Continents. *Journal of Virology*, *73*(1), 270 LP – 280. http://jvi.asm.org/content/73/1/270.abstract

Niegowska, M., Rapini, N., Biet, F., Piccinini, S., Bay, S., Lidano, R., Manca Bitti, M. L., & Sechi, L. A. (2016). Seroreactivity against Specific L5P Antigen from Mycobacterium avium subsp. paratuberculosis in Children at Risk for T1D. *PLOS ONE*, *11*(6), e0157962. https://doi.org/10.1371/journal.pone.0157962

Ojeda, J. J., & Dittrich, M. (2012). *Fourier Transform Infrared Spectroscopy for Molecular Analysis of Microbial Cells BT - Microbial Systems Biology: Methods and Protocols* (A. Navid (Ed.); pp. 187–211). Humana Press. https://doi.org/10.1007/978-1-61779-827-6_8

Ott, S. L., Wells, S. J., & Wagner, B. A. (1999). Herd-level economic losses associated with Johne's disease on US dairy operations. *Preventive Veterinary Medicine*, *40*(3), 179–192. https://doi.org/https://doi.org/10.1016/S0167-5877(99)00037-9

Park, H.-T., Shin, M.-K., Park, H.-E., Cho, Y.-I., & Yoo, H. S. (2016). PCR-based detection of Mycobacterium avium subsp. paratuberculosis infection in cattle in South Korea using fecal samples. *The Journal of Veterinary Medical Science*, *78*(9), 1537–1540. https://doi.org/10.1292/jvms.15-0271

Philalay, J. S., Palermo, C. O., Hauge, K. A., Rustad, T. R., & Cangelosi, G. A. (2004). Genes required for intrinsic multidrug resistance in Mycobacterium avium. *Antimicrobial Agents and Chemotherapy*, *48*(9), 3412–3418. https://doi.org/10.1128/AAC.48.9.3412-3418.2004

Pileri, E., & Mateu, E. (2016). Review on the transmission porcine reproductive and respiratory syndrome virus between pigs and farms and impact on vaccination. *Veterinary Research*, *47*(1), 108. https://doi.org/10.1186/s13567-016-0391-4

Prather, R. S., Rowland, R. R. R., Ewen, C., Trible, B., Kerrigan, M., Bawa, B., Teson, J. M., Mao, J., Lee, K., Samuel, M. S., Whitworth, K. M., Murphy, C. N., Egen, T., & Green, J. A. (2013). An intact sialoadhesin (Sn/SIGLEC1/CD169) is not required for attachment/internalization of the porcine reproductive and respiratory syndrome virus. *Journal of Virology*, *87*(17), 9538–9546. https://doi.org/10.1128/JVI.00177-13

Rahe, M. C., & Murtaugh, M. P. (2017). Mechanisms of Adaptive Immunity to Porcine Reproductive and Respiratory Syndrome Virus. *Viruses*, *9*(6), 148. https://doi.org/10.3390/v9060148

Rathnaiah, G., Zinniel, D. K., Bannantine, J. P., Stabel, J. R., Gröhn, Y. T., Collins, M. T., & Barletta, R. G. (2017). Pathogenesis, Molecular Genetics, and Genomics of Mycobacterium avium subsp. paratuberculosis, the Etiologic Agent of Johne's Disease . In *Frontiers in Veterinary Science* (Vol. 4, p. 187). https://www.frontiersin.org/article/10.3389/fvets.2017.00187

Ravva, S. V, Harden, L. A., & Sarreal, C. Z. (2017). Characterization and Differentiation of Mycobacterium avium subsp. paratuberculosis from Other Mycobacteria Using Matrix Assisted Laser Desorption/Ionization Time-of-Flight Mass Spectrometry. *Frontiers in Cellular and Infection Microbiology*, *7*, 297. https://doi.org/10.3389/fcimb.2017.00297

Rebuffo-Scheer, C. A., Kirschner, C., Staemmler, M., & Naumann, D. (2007). Rapid species and strain differentiation of non-tubercoulous mycobacteria by Fourier-Transform Infrared microspectroscopy. *Journal of Microbiological Methods*, *68*(2), 282—290. https://doi.org/10.1016/j.mimet.2006.08.011

Reiner, G., Fresen, C., Bronnert, S., & Willems, H. (2009). Porcine Reproductive and Respiratory Syndrome Virus (PRRSV) infection in wild boars. *Veterinary Microbiology*, *136*(3), 250–258. https://doi.org/https://doi.org/10.1016/j.vetmic.2008.11.023

Ricchi, M., Mazzarelli, A., Piscini, A., Di Caro, A., Cannas, A., Leo, S., Russo, S., & Arrigoni, N. (2017). Exploring MALDI-TOF MS approach for a rapid identification of Mycobacterium avium ssp. paratuberculosis field isolates. *Journal of Applied Microbiology*, *122*(3), 568–577. https://doi.org/10.1111/jam.13357

Rodriguez-Saona, L. E., Khambaty, F. M., Fry, F. S., & Calvey, E. M. (2001). Rapid Detection and Identification of Bacterial Strains By Fourier Transform Near-Infrared Spectroscopy. *Journal of Agricultural and Food Chemistry*, *49*(2), 574–579. https://doi.org/10.1021/jf000776j

Roiz, M. P., Palenque, E., Guerrero, C., & Garcia, M. J. (1995). Use of restriction fragment length polymorphism as a genetic marker for typing Mycobacterium avium strains. *Journal*

of Clinical Microbiology, *33*(5), 1389 LP – 1391. http://jcm.asm.org/content/33/5/1389.abstract

Rowland, R. R. R., Lawson, S., Rossow, K., & Benfield, D. A. (2003). Lymphoid tissue tropism of porcine reproductive and respiratory syndrome virus replication during persistent infection of pigs originally exposed to virus in utero. *Veterinary Microbiology*, *96*(3), 219–235. https://doi.org/https://doi.org/10.1016/j.vetmic.2003.07.006

Saleeb, P. G., Drake, S. K., Murray, P. R., & Zelazny, A. M. (2011). Identification of mycobacteria in solid-culture media by matrix-assisted laser desorption ionization-time of flight mass spectrometry. *Journal of Clinical Microbiology*, *49*(5), 1790–1794. https://doi.org/10.1128/JCM.02135-10

Sang, Y., Rowland, R. R. R., & Blecha, F. (2011). Interaction between innate immunity and porcine reproductive and respiratory syndrome virus. *Animal Health Research Reviews*, *12*(2), 149–167. https://doi.org/DOI: 10.1017/S1466252311000144

Santos, C., Paterson, R. R. M., Venâncio, A., & Lima, N. (2010). Filamentous fungal characterizations by matrix-assisted laser desorption/ionization time-of-flight mass spectrometry. *Journal of Applied Microbiology*, *108*(2), 375–385. https://doi.org/10.1111/j.1365-2672.2009.04448.x

Shapaval, V., Schmitt, J., Møretrø, T., Suso, H. P., Skaar, I., Åsli, A. W., Lillehaug, D., & Kohler, A. (2013). Characterization of food spoilage fungi by FTIR spectroscopy. *Journal of Applied Microbiology*, *114*(3), 788–796. https://doi.org/10.1111/jam.12092

Shapaval, V., Brandenburg, J., Blomqvist, J., Tafintseva, V., Passoth, V., Sandgren, M., & Kohler, A. (2019). Biochemical profiling, prediction of total lipid content and fatty acid profile in oleaginous yeasts by FTIR spectroscopy. *Biotechnology for Biofuels*, *12*(1), 140. https://doi.org/10.1186/s13068-019-1481-0

Shin, S. J., Lee, B. S., Koh, W.-J., Manning, E. J. B., Anklam, K., Sreevatsan, S., Lambrecht, R. S., & Collins, M. T. (2010). Efficient differentiation of Mycobacterium avium complex species and subspecies by use of five-target multiplex PCR. *Journal of Clinical Microbiology*, *48*(11), 4057–4062. https://doi.org/10.1128/JCM.00904-10

Singhal, N., Kumar, M., Kanaujia, P. K., & Virdi, J. S. (2015). MALDI-TOF mass spectrometry: an emerging technology for microbial identification and diagnosis. *Frontiers in Microbiology*, *6*, 791. https://doi.org/10.3389/fmicb.2015.00791

Sjöholm, M. I. L., Dillner, J., & Carlson, J. (2008). Multiplex detection of human herpesviruses from archival specimens by using matrix-assisted laser desorption ionization-time of flight mass spectrometry. *Journal of Clinical Microbiology*, *46*(2), 540–545. https://doi.org/10.1128/JCM.01565-07

Stadejek, T., Stankevicius, A., Murtaugh, M. P., & Oleksiewicz, M. B. (2013). Molecular evolution of PRRSV in Europe: current state of play. *Veterinary Microbiology*, *165*(1–2), 21—28. https://doi.org/10.1016/j.vetmic.2013.02.029

Sun, Haiyan, "Study of a Synthetic Porcine Reproductive and Respiratory Syndrome Virus Strain as a Vaccine Candidate" (2017). ETD collection for University of Nebraska - Lincoln. AAI10683682.

Tian, Z.-J., An, T.-Q., Zhou, Y.-J., Peng, J.-M., Hu, S.-P., Wei, T.-C., Jiang, Y.-F., Xiao, Y., & Tong, G.-Z. (2009). An attenuated live vaccine based on highly pathogenic porcine reproductive and respiratory syndrome virus (HP-PRRSV) protects piglets against HP-PRRS. *Veterinary Microbiology*, *138*(1), 34–40. https://doi.org/https://doi.org/10.1016/j.vetmic.2009.03.003

Van Breedam, W., Van Gorp, H., Zhang, J. Q., Crocker, P. R., Delputte, P. L., & Nauwynck, H. J. (2010). The M/GP(5) glycoprotein complex of porcine reproductive and respiratory syndrome virus binds the sialoadhesin receptor in a sialic acid-dependent manner. *PLoS Pathogens*, *6*(1), e1000730–e1000730. https://doi.org/10.1371/journal.ppat.1000730

Verheije, M. H., Kroese, M. V, van der Linden, I. F. A., de Boer-Luijtze, E. A., van Rijn, P. A., Pol, J. M. A., Meulenberg, J. J. M., & Steverink, P. J. G. M. (2003). Safety and protective efficacy of porcine reproductive and respiratory syndrome recombinant virus vaccines in young pigs. *Vaccine*, *21*(19), 2556–2563. https://doi.org/https://doi.org/10.1016/S0264-410X(03)00047-1

Vu, H. L. X., Ma, F., Laegreid, W. W., Pattnaik, A. K., Steffen, D., Doster, A. R., & Osorio, F. A. (2015). A Synthetic Porcine Reproductive and Respiratory Syndrome Virus Strain Confers Unprecedented Levels of Heterologous Protection. *Journal of Virology*, *89*(23), 12070 LP – 12083. https://doi.org/10.1128/JVI.01657-15

Wang, J., Moolji, J., Dufort, A., Staffa, A., Domenech, P., Reed, M. B., & Behr, M. A. (2015). Iron Acquisition in Mycobacterium avium subsp. paratuberculosis. *Journal of Bacteriology*, *198*(5), 857–866. https://doi.org/10.1128/JB.00922-15

Wang, L., Zhang, L., Huang, B., Li, K., Hou, G., Zhao, Q., Wu, C., Nan, Y., Du, T., Mu, Y., Lan, J., Chen, H., & Zhou, E.-M. (2019). A Nanobody Targeting Viral Nonstructural Protein 9 Inhibits Porcine Reproductive and Respiratory Syndrome Virus Replication. *Journal of Virology*, *93*(4), e01888-18. https://doi.org/10.1128/JVI.01888-18

World Organisation for Animal Health, W. (2008). *PRRS : the disease , its diagnosis , prevention and control*. *June*, 9–11.

Yoon, J., Joo, H. S., Goyal, S. M., & Molitor, T. W. (1994). A Modified Serum Neutralization Test for the Detection of Antibody to Porcine Reproductive and Respiratory Syndrome Virus in Swine Sera. *Journal of Veterinary Diagnostic Investigation*, *6*(3), 289–292. https://doi.org/10.1177/104063879400600326

Yu, X., Zhou, Z., Cao, Z., Wu, J., Zhang, Z., Xu, B., Wang, C., Hu, D., Deng, X., Han, W., Gu, X., Zhang, S., Li, X., Wang, B., Zhai, X., & Tian, K. (2015). Assessment of the safety and efficacy of an attenuated live vaccine based on highly pathogenic porcine reproductive and respiratory syndrome virus. *Clinical and Vaccine Immunology : CVI*, *22*(5), 493–502. https://doi.org/10.1128/CVI.00722-14

Yun, S.-I., & Lee, Y.-M. (2013). Overview: Replication of porcine reproductive and respiratory syndrome virus. *Journal of Microbiology (Seoul, Korea)*, *51*(6), 711–723. https://doi.org/10.1007/s12275-013-3431-z

Zhang, Q., & Yoo, D. (2015). PRRS virus receptors and their role for pathogenesis. *Veterinary Microbiology*, *177*(3), 229–241. https://doi.org/https://doi.org/10.1016/j.vetmic.2015.04.002

Zhang, Q., Guo, X., Gao, L., Huang, C., Li, N., Jia, X., Liu, W., & Feng, W. (2014). MicroRNA-23 inhibits PRRSV replication by directly targeting PRRSV RNA and possibly by upregulating type I interferons. *Virology*, *450–451*, 182–195. https://doi.org/https://doi.org/10.1016/j.virol.2013.12.020

Zuo, Y., Yuan, W., & Sun, J. (2015). Complete Genomic Characterization of Porcine Reproductive and Respiratory Syndrome Virus Strain HB-XL. *Genes*, *6*(3), 672–684. https://doi.org/10.3390/genes6030672

Zuo, Y., Yuan, W., Sun, J., Zhang, Q., Guo, X., Gao, L., Huang, C., Li, N., Jia, X., Liu, W., Feng, W., Yun, S.-I., Lee, Y.-M., Yu, X., Zhou, Z., Cao, Z., Wu, J., Zhang, Z., Xu, B., … Chae, C. (2013). Efficacy of a modified live porcine reproductive and respiratory syndrome virus (PRRSV) vaccine in pigs naturally exposed to a heterologous European (Italian cluster) field strain: Clinical protection and cell-mediated immunity. *Journal of Virology*, *6*(1), 289–292. https://doi.org/10.3390/genes6030672